Spring 2019

Effect of Cure Protocol on Network Formation and Properties of Epoxy-Diamine Thermosets

Andrew Janisse
University of Southern Mississippi

EFFECT OF CURE PROTOCOL ON NETWORK FORMATION AND PROPERTIES OF EPOXY-DIAMINE THERMOSETS

by

Andrew Patrick Janisse

A Dissertation
Submitted to the Graduate School,
the College of Arts and Sciences
and the School of Polymer Science and Engineering
at The University of Southern Mississippi
in Partial Fulfillment of the Requirements
for the Degree of Doctor of Philosophy

Approved by:

Dr. Jeffrey S. Wiggins, Committee Chair
Dr. William L. Jarrett
Dr. Sergei I. Nazarenko
Dr. Derek L. Patton
Dr. Robson F. Storey

Dr. Jeffrey S. Wiggins Committee Chair	Dr. Jeffrey S. Wiggins Director of School	Dr. Karen S. Coats Dean of the Graduate School

May 2019

Published by the Graduate School

ABSTRACT

The understanding of thermoset cure has, traditionally, been limited to the analysis of a single degree of cure value obtained via techniques such as dynamic scanning calorimetry (DSC). These analyses limit the scope of understanding of network development during cure. The continued development of rapid cure matrix chemistries necessitates the advancement of analytical techniques capable of quantifying how thermal cure profiles influence crosslinked network architectures throughout cure. This dissertation investigates and elucidates the mechanisms of polymer network growth through glassy epoxy/diamine thermoset to improve the way network growth is tracked and inform the role of cure protocol on network formation. The primary tool used to study the effect of cure protocol on network development was Real-Time Fourier Transform Infrared Spectroscopy in the near infrared wavelength region (RT-NIR).

Through the course of this work great strides were made in the considerations needed to accurately monitor functional group conversion in RT-NIR when using variable temperatures. A temperature dependence on the absorbance of NIR overtones was identified and a methodology to correct for the effect was developed. The improved RT-NIR analytical technique was applied to study how a thermal ramp rate affects the network formation pathway of high glass transition temperature (T_g), glassy thermosets during cure. It was determined that highly crosslinking networks based on the tetrafunctional epoxide tetraglycidyl-4,4'-diaminodiphenylmethane (TGDDM) have their pathway of network formation effected by the rate if thermal ramp to a constant cure temperature. Finally, the material properties of epoxy diamine networks cured with varied thermal ramp rate was studied. This dissertation improved upon the application of

RT-NIR as a quantifiable characterization tool to accurately study the formation of epoxy/diamine networks during cure. The RT-NIR technique was then applied to study a cure protocol effect on the pathway of network formation during cure of epoxy/diamine thermosets.

ACKNOWLEDGMENTS

I need to first and foremost thank my advisor, Dr. Jeffrey Wiggins. He has always supported and had faith in me even, and especially, when I didn't have faith in myself. By his leadership and deft touch, I have grown as a scientist, project manager, communicator, and as a person. I would not be here without Dr. Wiggins and I am eternally thankful for him.

I would like to sincerely thank my committee Dr. William Jarret, Dr. Sergei Nazarenko, Dr. Derek Patton, and Dr. Robson Storey. I am especially grateful to this committee always finding time in their schedules for me. Their selfless dedication to the students of this department is an inspiration to me.

The time I spent working on my doctoral research was made infinitely better to be performing it as a part of the Wiggins Research Group. WRG is defined by graduate students who go out of their way to help each other achieve. I want to thank every single person I worked with as a member of the group. It was always my ambition to return to the group something resembling the amount of help and support that the group gave me on countless occasions. While every WRG coworker I have had is valuable to me, I do feel compelled to mention a few specific people by name: Dr. John Misasi, Dr. Brian Greenhoe, and Dr. Andy Frazee; thank you for everything you did for me as I got my feet under me and learned how to be a productive member of this group. Jeremy Weigand and Jared Bates thank you for your friendship and for helping get across the finish line.

I owe a dept to every friend I have ever made at The University of Southern Mississippi. I am who I am because of you. I hope you had as much fun as I did.

Finally, I would like to acknowledge my father, Roland Janisse, for always expecting the best from me and for keeping me grounded through our weekly calls.

DEDICATION

Dedicated to my friends.

TABLE OF CONTENTS

LIST OF TABLES

LIST OF ILLUSTRATIONS

LIST OF ABBREVIATIONS

TGDDM	Tetraglycidyl-4,4'-diaminodiphenylmethane
DGEBF	Diglycidyl ether of bisphenol F
DGEBA	Diglycidyl ether of bisphenol A
33DDS	3,3’-diaminodiphenyl sulfone
44DDS	4,4’-diaminodiphenyl sulfone
T-33	TGDDM/3,3’-DDS mixture
T-44	TGDDM/4,4’-DDS mixture
F-33	DGEBF/3,3’-DDS mixture
WRG	Wiggins Research Group
DSC	Dynamic Scanning Calorimetry
FTIR	Fourier-Transform Infrared Spectroscopy
RT-FTIR	Real Time FTIR
NIR	FTIR in Near Infrared Region
T_g	Glass Transition Temperature
PALS	Positron Annihilation Lifetime Spectroscopy
DMA	Dynamic Mechanical Analysis
DIC	Digital Image Correlation
NMR	Nuclear Magnetic Resonance
SEC	Size Exclusion Chromatography
EEW	Epoxide Equivalent Weight
ΔH_{UC}	Total heat of reaction
ΔH_C	Residual heat of reaction

DOC	Degree of Cure
MDSC	Modulated DSC
DTGS	Deuterated triglycine sulfate detector
TMA	Thermomechanical Analyzer

CHAPTER I – INTRODUCTION

1.1 Aerospace Composites

The history of mankind has been defined by the innovation of material science. The development, use, and continued improvement of materials is so important that entire periods of time have been defined by the predominant material of use. The Stone Age, Bronze Age, and Iron Age have marked humanity's progress in the understanding of materials, thereby allowing the harnessing of their favorable properties.

It could very well be argued that we are currently living in the Polymer Age. The proliferation of polymers in the last century has promoted an explosion of new technologies as these synthetic materials have, in many cases, exceeded properties of their traditional analogs. The composite industry is on the leading edge of these technological innovations. A composite is a compound of two or more components that, when combined, provide properties and performance unattainable by the constituents. Polymer based composites have superior strength-to-weight ratios and corrosion resistance as compared to many metals. Thus, composites have replaced metals in industries such as: construction, commercial products, civil infrastructure, and transportation.

The advantages of composite materials are especially salient in the aerospace industry. Even small improvements in strength-to-weight ratio can result in large gains in fuel economy and aircraft performance. The continued development of this technology can revolutionize industrial materials as evidenced in the recent development of the Boeing 787 Dreamliner.

Aerospace composites are predominantly composed of carbon fiber reinforcement imbedded within a high glass transition temperature (T_g) epoxy network cured with a diamine hardener. The epoxy/amine network serves as the composite matrix transferring applied load to the fiber reinforcement. Delivering the thermal and mechanical properties necessary in aerospace applications requires epoxide and amine curatives that are typically aromatic, low-molecular-weight monomers, which cure around the reinforcement to form highly crosslinked networks. The industrial protocol used to cure composite panels has not been challenged. This is attributed to the final parts produced by these methods having properties that meet target benchmarks. There is much potential in terms of fundamental scientific knowledge as well as industrial economic benefit in understanding the role of cure protocols on the formation of composite-relevant, high T_g, glassy epoxy/amine networks. In fact, few studies have focused on this question in the published literature especially with the focus on the role of temperature ramp rates on network formation. Thus, this work examines this question, with an emphasis on network formation throughout cure via real time monitoring of functional group conversion and production.

1.2 Epoxy/Amine Networks

The leading matrix chemistries used in aerospace fiber reinforced composites are epoxy/amine thermosets. The epoxide/amine reaction involves the ring opening of the oxirane ring of the epoxide functional group by an amine via nucleophilic attack to generate a hydroxypropylether linkage.[1] A typical aerospace epoxy/amine network is formed by reacting an epoxide monomer (functionality ≥ 2) with an aliphatic or aromatic

diamine curative having two primary amine functional groups. This step-growth polymerization begins with the opening of the oxirane ring by the primary amine, creating a secondary amine and a hydroxyl site (Figure 1.1). For cures involving a difunctional epoxide, this first reaction phase is characterized by linear growth of the polymer. In the second phase, the secondary amine attacks another oxirane to form a crosslink between chains and creates tertiary amine group.[2,3] For epoxy networks composed of epoxide monomers of greater functionality (e.g. tetrafunctional), polymer branching and crosslinking occurs earlier in the reaction as compared to reactions involving difunctional epoxide monomers.[4,5]

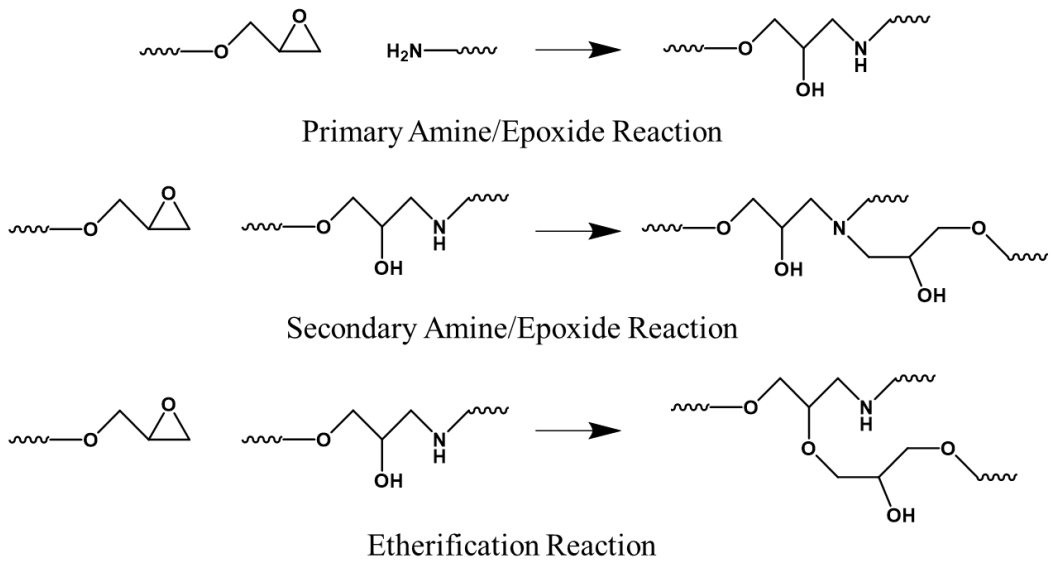

Figure 1.1 Prominent reactions in the epoxy/diamine network polymerization.

During network formation, the oxirane ring can also react with a hydroxyl group to form an ether linkage. This etherification reaction consumes a hydroxyl and an epoxide group but also produces a new hydroxyl group.[6,7] Etherification has a higher activation energy than the primary or secondary epoxide/amine reactions; thus this pathway has a

lower probability of occurrence. In general, for epoxy networks cured with aromatic diamines etherification occurs only after extended cure times and at elevated temperatures during the late stages of cure. In the literature, etherification has been driven in epoxy/amine networks by curing systems with an excess of epoxide so those groups were be available for reaction with free hydroxyls upon complete consumption of amine.[8] In systems prepared at 1:1 stoichiometry, etherification is commonly viewed to be a negligible event.[6,9]

Epoxy network cures are very complex because both the chemical and physical environment changes during polymerization, with the physical state of the system transitions from a liquid, to a gel, and finally to a glassy solid.[10–13] The liquid system at the beginning of cure has no molecular network present that restricts diffusion; the monomers can freely move in solution and react to each other. During this stage the molecular weight of oligomers increase, thereby increasing the system's overall viscosity. The size of isolated reacted species grows until a network spanning the entire sample forms. This is termed the point of gelation and is also considered the point where the molecular weight of the growing polymer is infinite.[14]

Although the gel is insoluble, it is surrounded by a soluble fraction consisting of lower molecular weight species and unreacted monomer. After gelation, network growth progresses as more of these monomers react and add to the system-spanning network. During this initial stage of network growth, the unreacted species can diffuse freely and react with the network, as functional group reactivity is unchanged from that in the liquid state.[15] The crosslink density of the system increases as the reaction proceeds, eventually

affecting the diffusion of branched segments that are not a part of the gel and eventually, even begin restricting diffusion of the unreacted monomer.[16]

The network continues to develop until the system reaches a glass transition temperature (T_g) that exceeds the cure temperature. This transition from a rubbery crosslinked system to an amorphous glassy network is termed the point of vitrification and represents the loss of long-range cooperative mobility of the backbone segments of the network. At this point the rate of crosslinking and functional group conversion is reduced as the cure kinetics become limited by diffusion.[17,18] Upon vitrification the developed network structure is effectively frozen. Further reactions can occur, advancing the degree of cure, but most of the network has already formed; limiting its impact on the overall network architecture. Networks which vitrify during the cure typically do not reach a fully cured state, meaning that not all the available functional groups (such as the epoxides) are reacted into the network. In order to reach full conversion, higher "post-cure" temperatures are applied, devitrifying the network to create the mobility necessary to react the remaining functional groups.[19,20]

The individual reactions occurring in epoxy/amine network formation are generally understood and have been verified via model systems and small molecule analogs. However, the kinetics and ordering of these reactions, and how they are affected by cure pathway is not well understood. In addition, the methods used to monitor cure kinetics are questionable. These are important issues as monomer connectivity directly affects ultimate network properties, with the manner these materials are cured greatly affecting the curing cycle time and cost of composite parts.

Network properties, especially in the glassy state, are related to several factors, including crosslink density, chemical composition between crosslinks, concentration of unreacted end groups, and structural defects.[21–24] Most of these factors are governed by the order of network-forming reactions, as this ultimately determines the architecture.[25] If all available primary amines react prior to any secondary amines or hydroxyls the evolution of the network structure will be much different than for cases where those reactions are more competitive. For thermoset matrix polymers, the term "network architecture" describes the three dimensional arrangement of monomers in space. The description of network architecture exists on the order of nanometers and the nature of these molecular orientations have been a focus of considerable work in the Wiggins Research Group (WRG) over the last several years.[26–29] The general hypothesis of this study is that the cure heating ramp rate dictates the kinetics of the various network reactions and therefore can be used to control cured network architecture.[30–32] Previous research in WRG has attempted to probe these differences by a variety of methods, including free volume measurements such as solvent uptake and Positron Annihilation Lifetime Spectroscopy (PALS), dielectric and spectroscopic analysis, dynamic mechanical analysis (DMA), differential scanning calorimetry (DSC), Digital Image Correlation (DIC) and even measurements of macro-scale properties such as ultimate mechanical performance.[33,34]

Network structure and the ultimate mechanical properties of a cured epoxy/amine thermoset are greatly influenced by the chemical structure of its component monomers. Subtle differences in structure of these building blocks significantly effect network

properties. For example, Diglycidyl ether of bisphenol-F (DGEBF) and diglycidyl ether of bisphenol-A (DGEBA) are almost identical in structure, both are based on bisphenols and difunctional. The only difference is that DGEBA has an isopropylidene moiety at the center of the molecule, whereas DGEBF has a methylene group in that position. Networks based on DGEBA have higher T_gs as compared to their DGEBF analogs directly because the isopropylidene moiety limits the molecular motion of the backbone.[26] A similarly dramatic effect is observed in the case of the two diaminodiphenylsulfone (DDS) structural isomers commonly studied as aromatic curatives in aerospace grade networks.[28] The meta-substituted isomer, 3,3'-DDS, has more conformational mobility than the para-substituted isomer, 4,4'-DDS. The increased backbone rigidity of systems cured with 4,4'-DDS leads to networks with higher T_gs and more robust mechanical properties.

Another major determinant on material properties of epoxy/diamine networks is the functionality of the epoxide monomer. Systems with higher functionality typically affect network architecture by increasing the crosslink density.[35] High-functionality monomers experience rapid growth in molecular weight, with the high crosslink density constraining molecular motion in the growing network. Higher crosslink density increases glass transition temperature; consequently, vitrification occurs earlier during the cure.[36] Cured multifunctional resins have the potential to create heterogeneous network architectures, with a range of crosslink densities throughout the network due to the limited mobility in these systems.[37]

Network architecture is related to the chemical structure and functionality of the epoxide and diamine monomers. The role of the pathway these systems take while forming the network's final structure is less understood. Epoxy/diamine thermosets can follow different reaction pathways. For example, all the primary amines may react prior to any secondary amines. For cases involving difunctional epoxides this would promote linear chain growth prior to significant branching and crosslinking.[38] The linear growth pathway is thought to produce more homogenous networks as the linear segments pack efficiently before crosslinking. Alternatively, if secondary amines react before the primary amine groups are exhausted, network formation will proceed in a "microgel-type" manner. Therefore, the relative reactivity of the secondary amines versus the primary amines has significant implications for network architecture.

During "microgel-type" growth, branching and crosslinking occur in portions of the developing network earlier in cure, creating localized regions of high crosslink density. As the cure progresses these regions impinge on one another to form a single network.[39] Microgel-type growth generally produces a more heterogenous network. The degree of network homogeneity can be qualitatively probed with DMA; indicated by observing the breadth of the tan δ peak at T_g, which is related to the uniformity of the viscoelastic response of a cured network.

1.3 Cure Protocol Dependence

Over the past half century, many factors affecting the ultimate material properties of epoxy/amine thermosets have been thoroughly investigated.[40–42] These include factors such as the chemical make-up of the network backbone as well as isomer effects and the

role of monomer functionality.[43] The role of the protocol utilized to cure these networks has received comparatively limited attention. As a result, there is little agreement in the literature on the effect variables such as cure temperature, isothermal dwell time, or temperature ramp rate have on network formation.[44–48] This lack of a consensus understanding is responsible for the varied methodologies used to address these questions. Most of the research in this area predominantly focus on final mechanical properties. It has been demonstrated that the study of final network properties can identify relationships between cure protocol and network formation. For example, Trappe and coworkers observed a connection between cure rate and the propagation of microcracks within a cured polymer matrix.[49,50] This was attributed to increasing levels of built up residual stress in the matrix after vitrification due to the restricted mobility of the network. However, only testing final material properties provides a limited scope of network formation as it ignores the development of network properties as cure progresses. Macroscopic tests also cannot adequately probe molecular level events during network formation. A complete study of thermoset cure necessitates the use of analytical techniques which can monitor network formation in real time throughout the reaction.

The most commonly used, and conventionally trusted, characterization tool for studying cure is DSC.[51] The magnitude and rate of evolution of the exothermic reactions can be directly monitored with DSC; so the cure event can be directly studied. It is understood that varying the maximum cure temperature alters the conversion and thermomechanical properties of the network by affecting the onset of vitrification.[52] The majority of the studies in this area focus on isothermal cures at a given temperature or

multiple, segmented isotherms at increasingly high temperature; however, it is unclear if the heating ramp rate affects the network formation pathway and/or the eventual material properties. Hardis and coworkers studied the effect of cure protocol for a difunctional epoxide and aliphatic amine system.[53] This system used is a relatively low temperature curing epoxy that does not form the high T_g glassy thermosets commonly used in high performance aerospace materials. However, it does serve as a platform for studying the cure throughout network formation. The project is notable for monitoring the development of the degree of cure over time through the course of reaction proceeds. In addition, the kinetics and non-isothermal behavior of the networks were mapped using DSC, Raman spectroscopy, and dielectric analysis. This work demonstrated the potential for *in situ* characterization techniques to record the evolution of cure and correlate the results with the more commonly accepted DSC data. It was found that the development of the network (i.e. the degree of cure) could be predicted for isothermal cure at various temperatures. However, the utility of *in situ* monitoring of network growth in a thermally dynamic environment still requires validation.

There is great potential in understanding the role of temperature ramp rate on network formation. It would, obviously, provide increased theoretical understanding of epoxy/amine network cure, but there would also be a very real practical benefit. There is an inherent drive in the composites industry to expedite part turnover. Increased temperature ramp rates for the curing of thermosetting polymer networks reduces cycle time, especially as novel out-of-autoclave technologies continues to push the industry standards.[54–56] Understanding the effects of temperature ramps is also valuable for

industries desiring to maintain traditional and conservative cure protocols. As the composite industry continues to make inroads to the sectors of large-scale infrastructure and vehicle manufacturing, fabricated parts will continue to get larger and thicker. These thickset parts will heat unevenly from the surface into the interior, creating sections of the same part which experience differing thermal histories as the entire part reaches the cure temperature. Therefore, it is imperative to understand the role varied cure pathways have on final network properties.

1.4 Real-Time Near Infrared Spectroscopy

The development of an epoxy/amine network is difficult to monitor by many traditional polymer characterization techniques such as nuclear magnetic resonance (NMR) and size exclusion chromatography (SEC) due to the insoluble nature of the evolving thermoset. However, the progress of cure can be directly measured throughout the reaction by techniques such as DSC and rheology. These two methods, however, are only able to give information about the extent of cure in terms of a single number. It is difficult to infer any information on the developing network architecture by these techniques as they do not distinguish between the types of reactions occurring during cure. Real-Time Fourier-transform infrared spectroscopy (FTIR) spectroscopy has emerged as an invaluable tool for understanding how a network forms.[57]

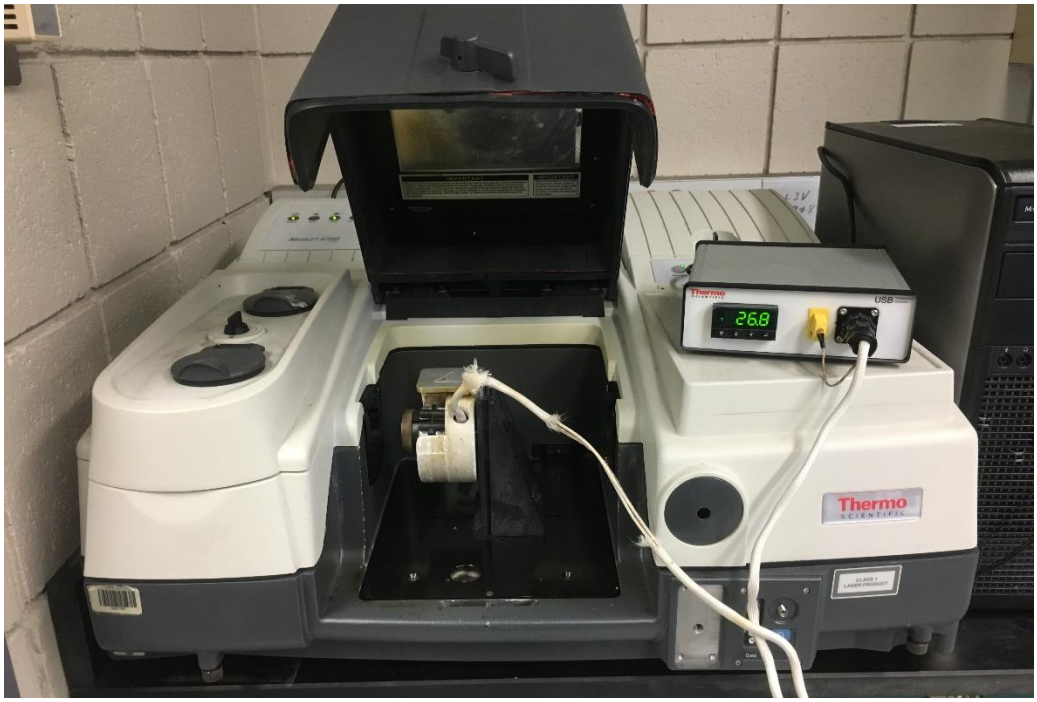

Figure 1.2 WRG Nicolette 6700 FTIR equipped with heated transmission cell.

The near infrared region (NIR) from 8000 cm^{-1} to 4000 cm^{-1} is used in this work because it contains overtones representative of the key functional groups in the epoxide/diamine reaction. Utilizing this region allows for the clear analysis of discrete absorbance peaks as opposed to using the mid-IR range (4000 cm^{-1} – 600 cm^{-1}) wherein the epoxide peak is only present within the so called "finger print" region which adds a high degree of complexity to deconvolute and accurately study the signal.[58–60] NIR spectroscopy is able to differentiate between the reaction of epoxides with primary and secondary amines and also monitor the production and consumption of hydroxyl groups.[61,62] This allows monitoring of network structure from the earliest state of the reaction in the liquid phase, through gelation, vitrification, and beyond.

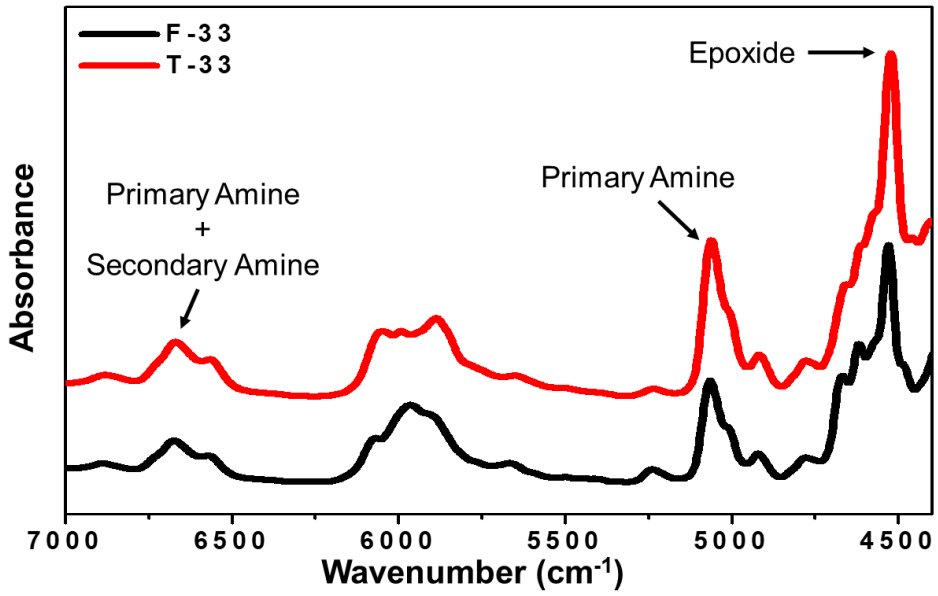

Figure 1.3 Initial spectra for two different epoxy/diamine with relevant peaks identified.

In infrared spectroscopy chemical structures (such as functional groups) absorb the incident light at specific frequencies which match the vibration frequency of specific groups. Because of this, the presence of functional groups can be discerned by their characteristic absorbance at known frequencies. The total absorbance of a given species at a specific wavenumber is directly related to the light which interacts with the sample as can be observed in equation 1.1.[63,64] The term 'A' here is absorbance, I_0 is the intensity of radiation entering the sample, and I is the intensity of radiation upon leaving the sample picked up by the detector.

$$A = log_{10}(I_0/I) \quad \text{[Equation 1.1]}$$

FTIR spectroscopy commonly is used qualitatively to determine the presence or absence of chemical groups, but in addition, the instrument can be used to quantitatively measure the consumption and production of key functional groups of a reaction. Here

NIR spectroscopy is especially useful in epoxy/diamine cures as the peaks of interest are well resolved.[65–67] Figure 1.3 illustrates two different epoxy/diamine systems an shows that the frequency of the absorption of the epoxide groups is unaffected by system composition.

The general method to determine the conversion of functional groups of interest during a reaction is described as follows: The peak at 5070 cm^{-1} is solely representative of primary amine and thus can be directly integrated to determine conversion over time. Conversion can be determined using the initial area of the peak of interest (A_0) and the peak area at some later time (A_t) using Equation 1.2. The primary amine for DDS, a key aerospace curative, also absorbs infrared at the wavenumbers 4535 cm^{-1} and 6680 cm^{-1}, which are the locations of the representative peaks for epoxides and secondary amines respectively. Interpretation of the peaks at those wavenumbers is more complicated, as the contribution from each functional group must be determined. This issue is addressed using Beer's law (Equation 1.3), where ε is the component's absorption coefficient (a constant directly pertaining to the functional group at a specific wave number), c is the concentration, and l is the path length.[68,69] The path length is typically normalized with the use of an internal standard; in these cases ε and l can be combined into a single term known as molar absorptivity (a). In NIR spectra the total absorbance of a band of more than one component is simply the sum of the individual components (Equation 1.4). The epoxide group exhibit a strong band at 4535 cm^{-1}, and the initial epoxide concentration of epoxide at the initial time is known, however in order to calculate epoxide conversion over time the portion of the absorbance signal from the primary amines must be

accounted for. The amine concentration at any given time can be obtained from the peak at 5070 cm^{-1}, thus the instantaneous concentration of epoxides can be directly studied by using the molar absorptivity term for each functional group at 4535 cm^{-1}.[70] Historically, the molar absorptivity term shown in Equation 1.3 is considered to be a constant.[71] This is acceptable when IR cure studies of epoxy systems are performed by removing the curing network from a separate vessel and performing IR scans on the sample at discreet time points all at room temperature. Additionally, the use of a single molar absorptivity constant is acceptable during *in situ* isothermal cure studies wherein the absorptivity was determined at the target temperature previously. Molar absorptivity can most accurately be described as a constant for a functional group at a specific wavenumber when studies are performed under the conditions at which it was measured.

$$\%\ Conversion = \left(\frac{A_0 - A_1}{A_0}\right) \times 100 \quad \text{[Equation 1.2]}$$

$$A = \varepsilon c l = a c \quad \text{[Equation 1.3]}$$

$$A_{total} = A_1 + A_2 = (\varepsilon_1 c_1 + \varepsilon_2 c_2) l \quad \text{[Equation 1.4]}$$

Methods for monitoring the epoxide/diamine cure via NIR spectroscopy have continuously improved.[72–75] Initially, cure studies had to be performed in a step-wise manner involving curing networks to increasing degrees of cure in an oven and then removing them for a single snapshot scan of the system.[76,77] With improved technology came the development of transmission cells which could impart heat to a sample while remaining in the beam path continually. This allowed for a proliferation of studies utilizing real-time near infrared (RT-NIR) data to improve the understanding of network

evolution. However, the vast majority of epoxy/diamine cure studies have focused on RT-NIR monitoring of isothermal cure conditions. Almost no investigations have analyzed epoxy networks cured with differing thermal ramp rates. It is also important to note, that there have been no reports on the effect of changing the thermal environment during data collection on the RT-NIR spectroscopic signal.[57,58,78–83]

1.5 Research Preview

This dissertation will investigate and elucidate the mechanisms of polymer network growth in glassy epoxy networks in order to improve methods to monitor network growth and establish the role of cure protocol on network formation. This work will increase the understanding of the effect of cure profiles for glassy, high T_g thermosets on network properties, which ultimately will impact the performance of industrially relevant, composite structures.

This dissertation focuses the role of thermal ramp rate in cure protocols of epoxy/diamine networks. The primary tool used in this study is RT-NIR spectroscopy. Through the course of this work significant improvements were made in the techniques needed to accurately monitor functional group conversion in RT-NIR, especially under variable temperature conditions. Chapter III focuses on these improvements with a special emphasis on the identification of the temperature dependence of molar absorptivity, which must be considered during analysis. Chapter IV studies the effect of cure protocol on network formation by analyzing the order of functional group consumption and production during epoxy/diamine cures. The role of isomerism of epoxy/diamine curatives as well as the degree of crosslinking are reported. Chapter V

will continue the study of cure protocol on viscoelastic and mechanical properties of fully cured and under cured networks. Finally, Chapter VI will contain concluding remarks as well as proposed areas for future work in this field.

CHAPTER II - EXPERIMENTAL

2.1 Material Preparation

Diglycidyl ether of bisphenol F (DGEBF) (Epon^{TM} Resin 862, Hexion Inc.) with an epoxide equivalent weight (EEW) of 165-173 g/epoxide or tetraglycidyl-4,4'-diaminodiphenylmethane TGDDM (Araldite MY721, Huntsman Chemical Company, EEW: 111-117 g/epoxide) was cured with 3,3'-diaminodiphenyl sulfone (33DDS) or 4,4'-diaminodiphenyl sulfone (44DDS). All networks were formulated using a 1:1 stoichiometric equivalent of oxirane to amine active hydrogen. All epoxy/amine mixtures were then heated at a prescribed rate to 180 °C, followed by a two-hour isotherm. Tested temperature ramp rates included: 0.5, 1, 3, 5, 10, and 20 °C/min. 40 °C/min was also investigated for some tests. TGDDM/33DDS formulations will be referred to in this document by the abbreviation T-33. T-44, similarly, will refer to TGDDM/44DDS, and F-33 for DGEBF/33DDS systems.

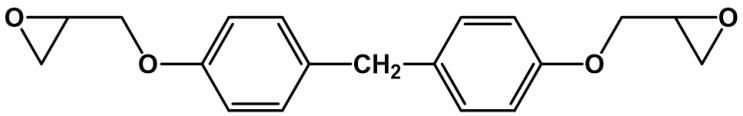

DGEBF
Diglycidyl Ether of Bisphenol F

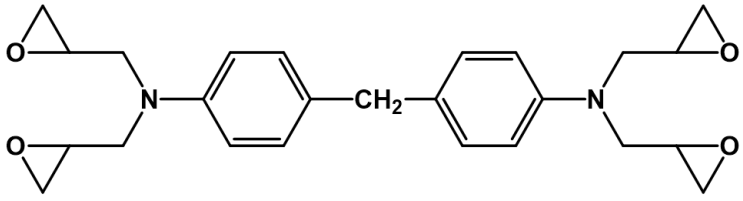

TGDDM
Tetraglycidylether of 4,4'-diaminodiphenyl methane

Figure 2.1 Epoxide monomers common to high T_g aerospace networks used in this work.

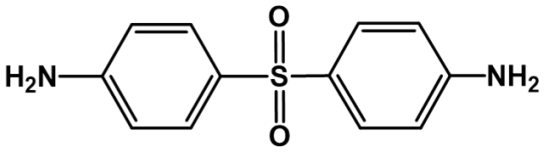

3,3'-DDS
3,3'-Diaminodiphenylsulfone

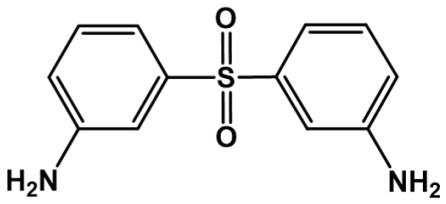

4,4'-DDS
4,4'-Diaminodiphenylsulfone

Figure 2.2 Diamine curatives used in this work.

For some portions of this work preparation of the epoxy/amine mixtures prior to cure was compared using the *traditional* WRG method. Most of the networks were cured from and studied beginning from a *slurry* state. The differences of the two methods are listed below.

The *traditional* method of network preparation in WRG would involve TGDDM being charged to a 500 mℓ Erlenmeyer flask equipped with a vacuum fitting and magnetic stirring device. The epoxide monomer would be heated to ~100°C with a stoichiometric amount of dried 33DDS or 44DDS slowly added over a 10 to 15 minute period to avoid agglomeration. Upon addition, vacuum was applied to a level of ~ -30 in Hg with the temperature increased to 125 °C in 5 °C intervals while the mixture stirred until dissolution of amine was observed. Vacuum was then removed and the clear solution either poured into preheated (100 °C) silicone molds of various dimensions for curing, or quenched at sub-ambient temperature for subsequent analysis.

The *slurry* method was determined to be favorable for the purposes of this study. Data supporting this is provided below. For this method a slurry of TGDDM or DGEBF and DDS (both 33 and 44) which had been combined in stoichiometrically equivalent amounts and prepared to homogeneity were mixed in a centrifugal speed mixer. Slurries were stored at sub ambient temperatures and were prepared in small volume batches to keep the mixtures used as fresh as possible.

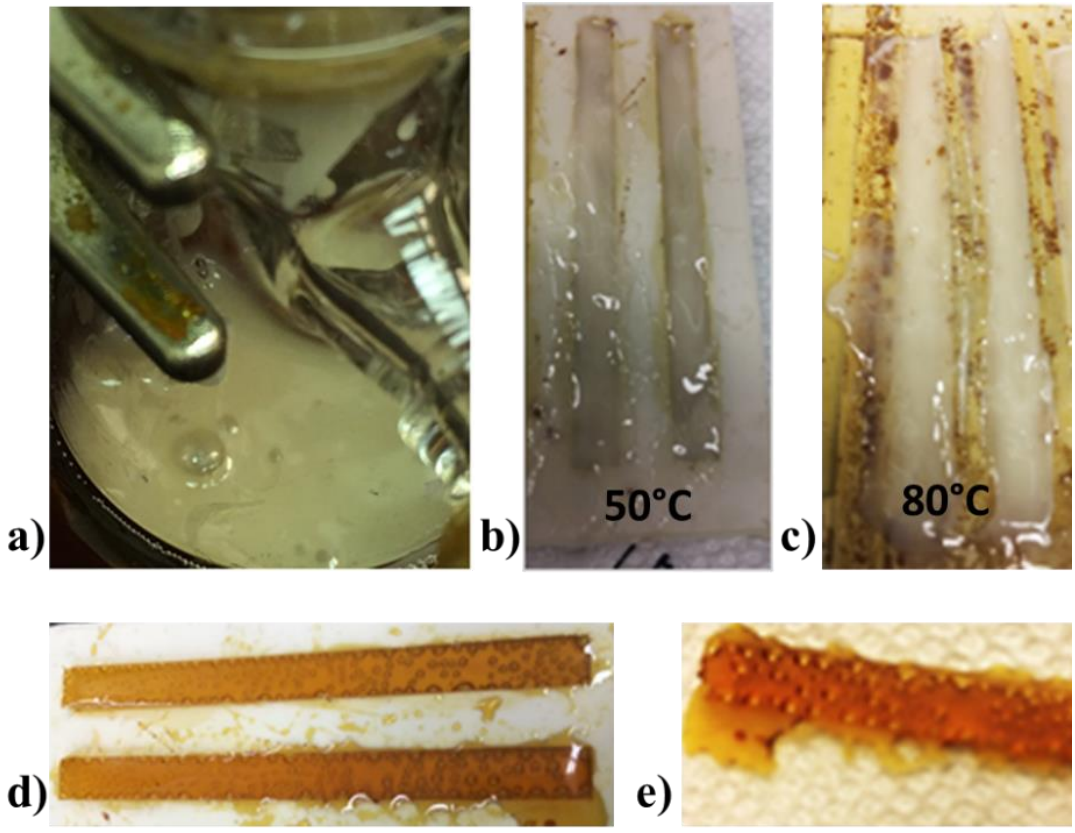

Figure 2.3 Sample molding issues when curing from slurry at low temperatures. a) degassing in Erlenmeyer flask, b) and c) filling the mold will slurry preheated to 50 and 80 °C respectively, d) and e) poor samples produced by the Erlenmeyer flask slurry method.

Due to the difficult workability of the slurried mixtures (Figure 2.3), material was placed in a vacuum oven preheated to 80°C to lower the viscosity. Vacuum (~-30 in Hg) was then applied to de-gas the mixture prior to molding. The material was then molded in

whichever shape required. If silicon molds were used (as shown in Figure 2.4) the molds were preheated to ~80°C to allow for the slurry to fill the molds.

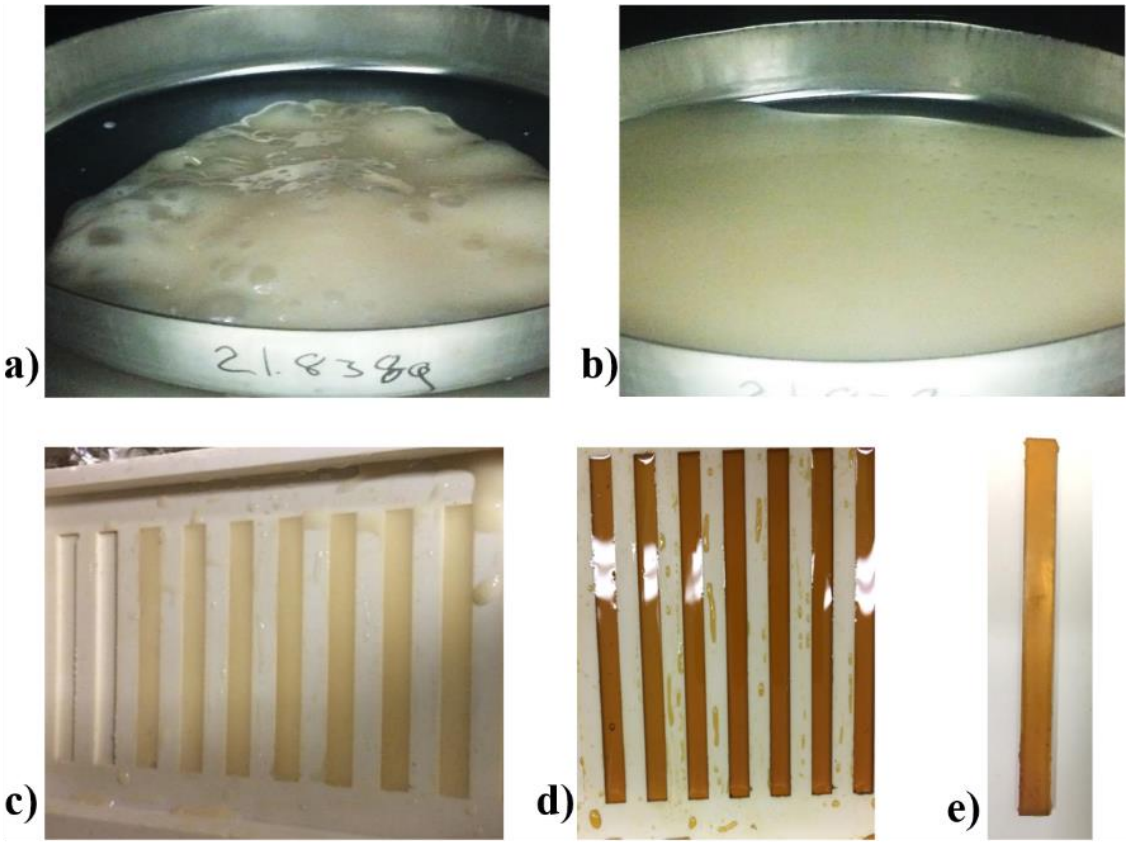

Figure 2.4 Slurry method for molding a) low viscosity slurry during degassing, b) after degassing, c) slurry poured into preheated DMA mold, d) mold after curing, e) close up of defect free DMA bar made using slurry method.

2.2 Differential Scanning Calorimetry (DSC)

The methods described in Material Preparation were used to mix the epoxy (TGDDM) and curative (33DD or 44DDS) for the DSC study, which was performed with a TA Instruments Q200 DSC. Homogenous, uncured material was further solidified by placing into liquid nitrogen to improve the ease of sample preparation. The cryogenic-temperature mixture was chipped into 2-6 mg sections and sealed into hermetic DSC pans. Two different cure prescriptions were used, one to obtain the total heat of reaction

of the uncured specimen (ΔHUC), and another to obtain the heat of reaction of a desired cure profile (ΔHC). The prescription for finding ΔHUC for each network formulation was a ramp at a set heating rate from -25 °C – 300 °C at 10°C/min. The residual heat of reaction (ΔHC) for any cure protocol was determined by the following method: a heat/isotherm/cool/heat prescription was used for any given heating rate up to isothermal hold at 180 °C for increasing durations, then the sample was cooled from 180 °C to -25 °C at 10 °C/min to halt the reaction, finally a second ramp of 10 °C/min to 300°C was applied and the heat of reaction exotherm collected and compared to the overall ΔHUC. Figure 2.5 represents the cure prescriptions used to obtain ΔHC for each ramp rate.

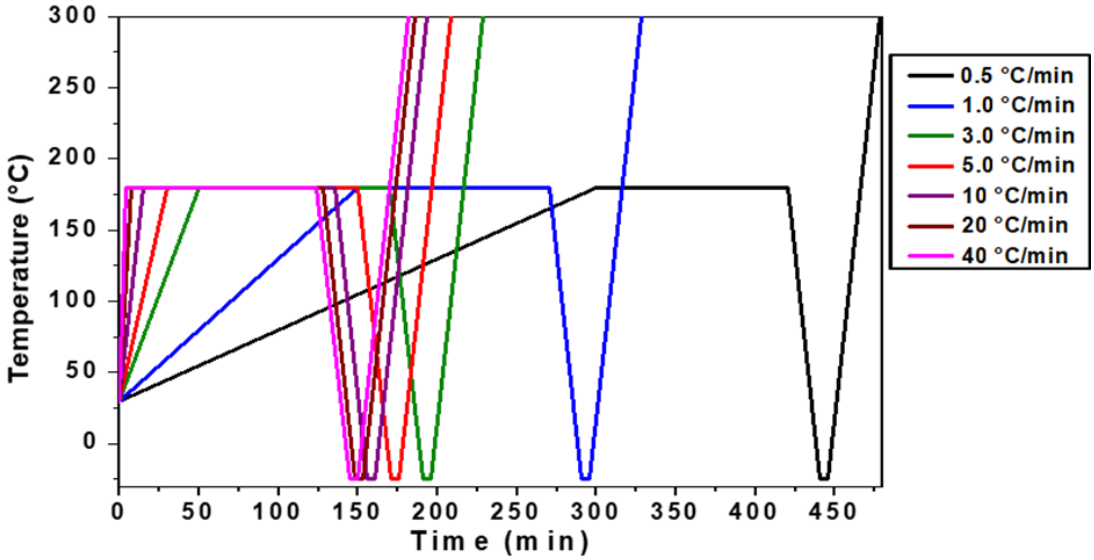

Figure 2.5 Thermal profile used in DSC cure studies of various cure protocols.

Degree of cure (DOC) was calculated from DSC data using Equation 2.1, where ΔHUC (J/g) is found by integration of the exotherm peak of the ΔHUC ramp, and ΔHC (J/g) is found by integration of the exotherm peak from the second ramp in the heat/cool/heat experiment.[84]

$$DOC = \frac{\Delta HUC - \Delta HC}{\Delta HUC} \times 100$$ [Equation 2.1]

2.3 Modulated Differential Scanning Calorimetry (MDSC)

The methods described in ***Material Preparation*** were used to mix and solubilize the epoxy (TGDDM) and curative (33DDS or 44DDS) for the MDSC study, which was performed with a TA Instruments Q2000 DSC. Homogenous, uncured material was further solidified by placing into liquid nitrogen to improve the ease of sample preparation. The cryogenic-temperature mixture was chipped into 2-6 mg sections and sealed into hermetic DSC pans. Modulated DSC tests were performed similarly to DSC where the slurry was ramped at a given rate to 180°C and held for a predetermined isotherm before being rapidly quenched to -25°C and then ramped to 300°C at 10°C/min in order to determine the residual exotherm as well as the T_g of the network which was formed by the given cure prescription.

MDSC differs from standard DSC in its ability to separate reversible and irreversible transitions by applying a sinusoidal heating rate as observed in Figure 2.6a. Slight changes in the rate of heating allow the instrument to identify and separate out reversible and irreversible transitions. This is of value for the present study because the T_g transition is reversible and the exotherm produced when finishing the residual cure is an irreversible transition. The residual exotherm in a standard heat flow graph can obscure the T_g making it difficult to monitor the progression of T_g along with the evolution of cure (Figure 2.6b).

For this project, both oven-cured samples and samples cured in the MDSC, were studied. In situ cured samples were ramped at a given rate and held for a predetermined isotherm, then quenched to -25°C and ramped at 10°C/min to 300°C with a modulation of

1°C every 60 sec. Samples which had previously been cured in the oven were just ramped from -25°C to 300°C at the same rate and with the same modulation in order to determine the properties of the network as it came out of the oven.

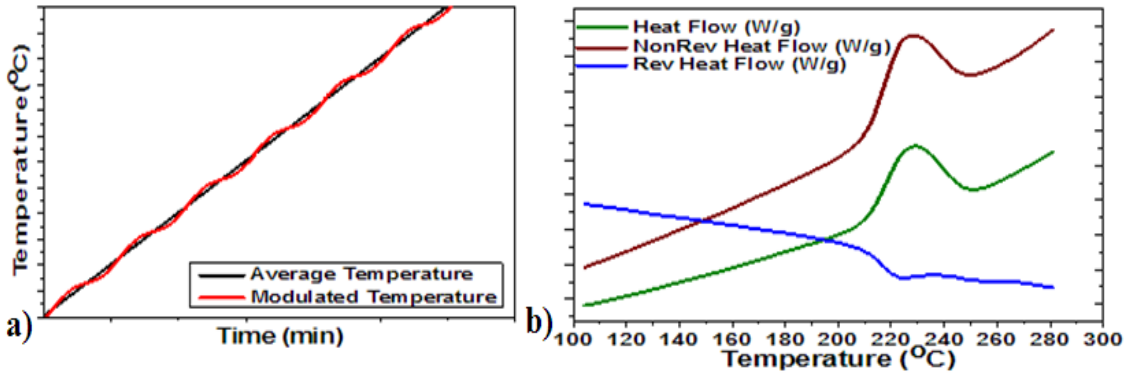

Figure 2.6 MDSC example output a) Sinusoidal modulated temperature applied during ramp, b) Heat flow separated into reversible and nonreversible signals.

2.4 Dynamic Mechanical Analysis (DMA)

Dynamic mechanical analysis experiments were conducted on a TA Instruments Q800 using a film tension test fixture. DMA specimens were formed by casting homogenized prepolymer into silicone molds with rectangular cavities of 5.0mm width by 1.5mm depth and 60.0mm length, and each cured with a prescribed cure schedule previously mentioned. After cure, specimens were trimmed to approximately 25mm in length, ensuring constant thickness and lack of voids or bubbles. Samples were then mounted in the three point bend clamp with a constant tested length of 20mm. A temperature sweep was used to develop E' and Tan δ vs. temperature relationships. A strain of 0.05 and a frequency of 1 Hz were used. Temperature sweeps were performed from 30 to 325 °C for standard investigation and lower temperatures (-125°C) were also studied to investigate sub T_g transitions. All thermal sweeps in these DMA tests were ramped at 3°C/min.

2.5 Near Infrared Spectroscopy

Fourier transform infrared spectroscopy in the near infrared range (4000-8000 cm^{-1}) in transmission mode was used to monitor network formation during each cure prescription studied. The *slurry* method described in ***Material Preparation*** was used to mix the epoxy (TGDDM or DGEBF) and curative (33DDS or 44DDS) for the near-infrared spectroscopy (NIR) study. The low viscosity epoxy/amine mixture was placed between two glass cover slides and within the confines of a steel washer (~1 mm thickness) in order to provide a constant thickness of the sample even during heating. The washer was adhered to the glass slides using a high temperature silicone-based gasket maker and allowed to set overnight to provide a good seal. The light source within the near infrared range is white light; this means optical clarity is necessary for the instrument to record a spectrum. Samples were exposed to the minimum amount of energy from a heat gun required to solubilize the curative into the epoxy and achieve clarity.

Experiments were performed using a Nicolet 6700 FT-IR from Thermo Fisher Scientific using a CaF_2 beamsplitter and deuterated triglycine sulfate detector (DTGS). Prepared samples were heated in a HT-32 Heated Transmission Cell from Simplex Scientific. The Simplex software was paired to the OMNIC FTIR software native to the Nicolet 6700. This allowed for various cure protocols to be performed while NIR transmission spectra were simultaneously recorded. A unique spectrum made of 32 scans (4 cm^{-1} resolution) was collected every minute to track the progress of the network formation.

2.6 Rheology

Oscillatory temperature ramp tests that mimicked the NIR cure profiles were performed on an ARES G2 Rheometer equipped with a forced air convection oven to determine the time to gelation for each cure protocol. Sample slurries were loaded onto smooth 25 mm aluminum parallel plates held at 30 °C and brought to a 1 mm plate gap. This gap was maintained in the pre-gelled state while a 10% oscillatory strain was imposed on the sample at a frequency of 1 Hz until gelation occurred, taken as the G' and G'' crossover. T-33 samples were brought through the entirety of cure (past gelation) on 8 mm aluminum plates to keep the forces imposed on the instrument below the point where damage could be done to the instrument to discern whether cure path variations could be observed. For these tests, a manually set change in strain was programmed to occur post gelation to prevent damaging the formed network, the initial pre-gel strain of 10% was dropped to 0.015% and an auto-strain feature was enabled that allows the software to vary the strain to protect the instrument. In conjunction with the strain change, the sample gap was allowed to change post-gelation to maintain a constant axial force as cure induced shrinkage occurred that would otherwise max out the axial transducer. The experiment was broken up into two steps, pre-gelation and post-gelation, to balance meaningful data acquisition and instrument safety due to the magnitude of viscosity and modulus development from the viscosity well in the liquid stage to the modulus plateau after vitrification.

2.7 Solvent Uptake

Solvent uptake tests are important validations to make before selecting a material for a service environment.[85] Highly crosslinked networks are often very resistant to

solvents. However, fluid uptake causes a plasticization effect in cured thermosets which decrease ultimate network properties.[86] Therefore, the effect of cure protocol on solvent uptake was probed in this work for fully cured networks. Samples were placed in deionized water and heated to reflux for 24 hours to expedite solvent swelling. The samples were recovered and dried and had their mass recorded (m_i) and the percent mass increase was calculate as shown in Equation 2.2. The sample geometry was 15mm x 5mm x 2mm.

$$\%\, mass\ increase\ = (m_i - m_0)/m_i \times 100 \quad \text{[Equation 2.2]}$$

CHAPTER III – IMPROVEMENTS IN THE QUANTIFIABILTY OF RT-NIR SPECTROSCOPY

3.1 Chapter Overview

Through the course of this dissertation work, a major development was made in using RT-NIR spectroscopy for quantitative analysis of cure in thermoset systems, namely the effect of temperature on molar absorptivity. This is especially important when analyzing the formation of a network during a nonisothermal cure. A simple correction factor for functional group absorptivities when at elevated temperatures was implemented. This dramatically improved the reliability of molar concentration data for the reactive species, needed to accurately ascertain the pathway to network formation. This chapter will show clear evidence of the temperature effect on absorbance and the need to apply a correction factor.

In order to obtain reliable data to monitor cure, other improvements to the technique had to be made. This chapter will begin with a description of some of these improvements prior to detailing the implementation of the temperature dependent absorptivity term.

3.2 Refinement of RT-NIR Technique

The Wiggins Research Group historically used RT-NIR spectroscopy to monitor epoxy/diamine cures.[26,27] These techniques were able to produce good, but inconsistent results. The frustrations associated with the technique ultimately led to an investigation of how the existing methodologies could be improved.

Analysis of epoxide/amine formulations in the NIR spectroscopic studies benefit from the fact that glass is invisible in the near infrared region, allowing samples to be

prepared using inexpensive materials. The absorbance signal for IR spectroscopy is directly related to the path length of the interacting radiation through a sample. It is therefore important, to the extent possible, to maintain a constant sample thickness in the direction parallel to the instrument beam. To try and achieve this, a method was developed in the research group of putting a drop of a solubilized and partially reacted epoxide/amine mixture between two glass slides separated by a spacer. The method involved affixing a thin Teflon ring to one glass slide with glue and then adding the drop of epoxy/amine solution to fill the ring followed by gluing the other side of the ring to a second glass slide. The heated cell used in the WRG FTIR instrument places the sample vertically (Figure 1.2), with the instrument beam traveling horizontally through the sample chamber. This instrument design, coupled with the glass/glue/Teflon sample cell assembly, led to many issues related to sample leakage. The effect of material leakage on a spectrum is shown in Figure 3.1. The path length changes dramatically which also affects the absorbance signal. Also, the appearance of air bubble passing through the beam path during cure creates sufficient noise to make proper analysis of an IR spectrum untenable.

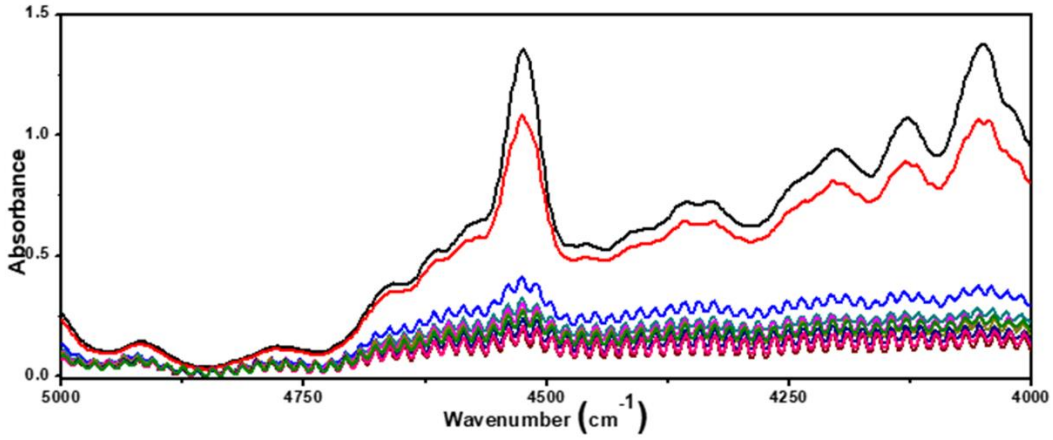

Figure 3.1 Stacked spectra during cure with original WRG IR sample preparation leading to leakage and unusable data.

Several improvements in sample preparation for the RT-NIR studies were developed which led to an increase in the consistency and reliability of the data. This led to a reduction in failed samples and allowed for a greater number of experiments to be analyzed. One improvement was changing the materials used in sample cell construction. A rigid steel washer was used as the spacer in the sample cell. Additionally, it was observed that the glue used to adhere the spacer to the glass windows was clear, which could lead to incomplete sealing via operator error and create a channel the curing system to leak out. Therefore, a high temperature grade silicon base gasket maker was used. The gasket maker was colored, making it easier to ensure complete coverage could be assured when making sample cells, also the steel washer and silicon sealant have low thermal expansion at the temperatures most commonly probed for cure studies further reducing the possibility of leaks.

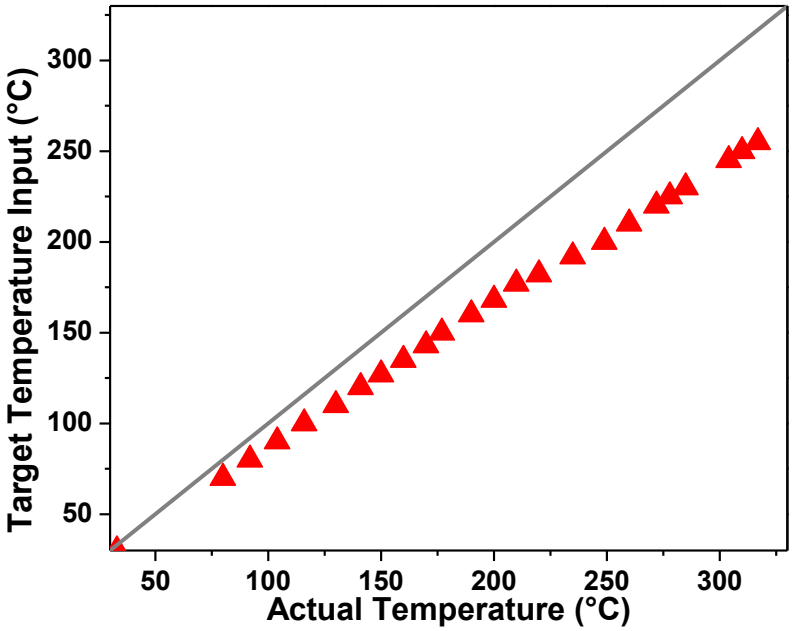

Figure 3.2 Actual temperature of the IR sample as related to the target input in heated cell program.

The analysis of cure data was also improved by identifying an offset between the targeted temperature of and the actual sample temperature. A sacrificial sample was prepared with a thermocouple embedded into an epoxide/amine slurry. Temperature versus time was recorded with an OMEGA HH147U data logger. Interestingly, the offset was consistent and linearly increased as the target temperature increased (Figure 3.2) This permitted the use of a straightforward correction to cure samples at the correct temperatures and ramp rates.

Figure 3.3 NIR sample made with slurry before and after solubilization.

As explained in Chapter II, in this work, a large emphasis was placed on studying network development from as close to a “true zero” degree of cure as possible. The primary strategy to achieve this was to begin the cure from a slurried state rather than after a solubilization step, which was known to cause some progression in the reaction. Monitoring cure via RT-NIR spectroscopy is not possible, however, when starting from a slurried state. The radiation source for the near infrared range is white light; therefore, optical clarity is necessary to detect a signal. Slurry loaded samples were slightly warmed with a heat gun for the minimum amount of time necessary for the curative to solubilize into the epoxy and clarify (Figure 3.3). Heat of reaction studies were performed on the mixtures before and after achieving optical clarity by this method and it was determined that no reaction occurred. As seen in Figure 3.4, no change in the cure exotherm of T-33 or F-33 (558.3 J/g and 402.1 J/g respectively) was observed after clarification.

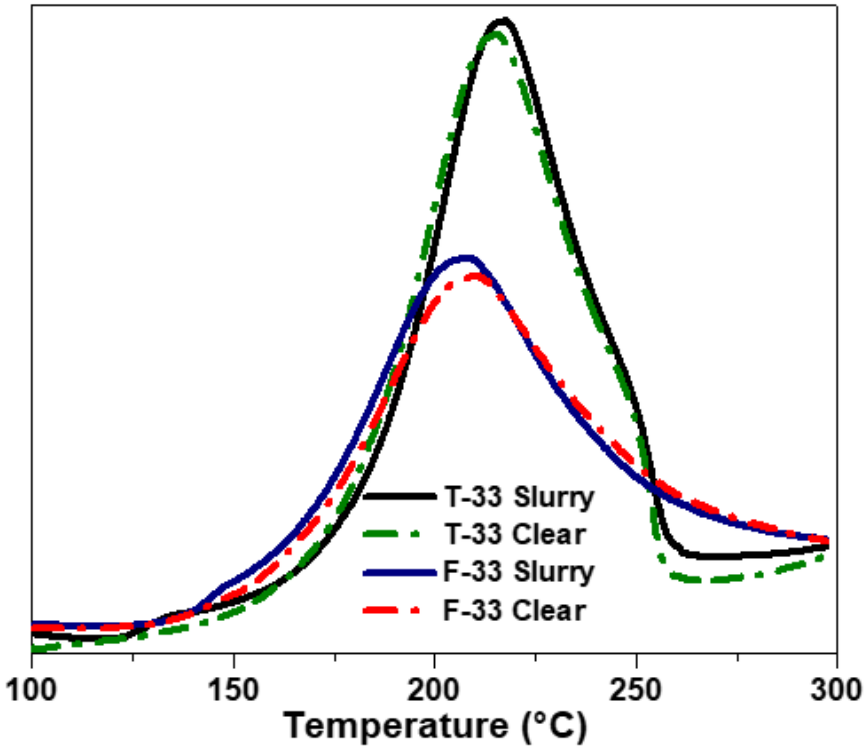

Figure 3.4 Exotherm of ΔHUC for T-33 and F-33 before and after clarification for IR.

Due to these practical improvements in acquiring data, consistent RT-NIR cure studies were now possible, allowing for in-depth studies of cure protocol on network formation. The ability to monitor the consumption of functional groups from as close to the beginning of cure as possible allows a more complete picture of the nature of the epoxy/diamine thermosetting reaction during cure to be drawn.

3.3 Temperature Dependence of Molar Absorptivity

An example of RT-NIR cure study data is shown in Figure 3.5. Select spectra have been selected to observe the evolution of the predominate peaks throughout cure.

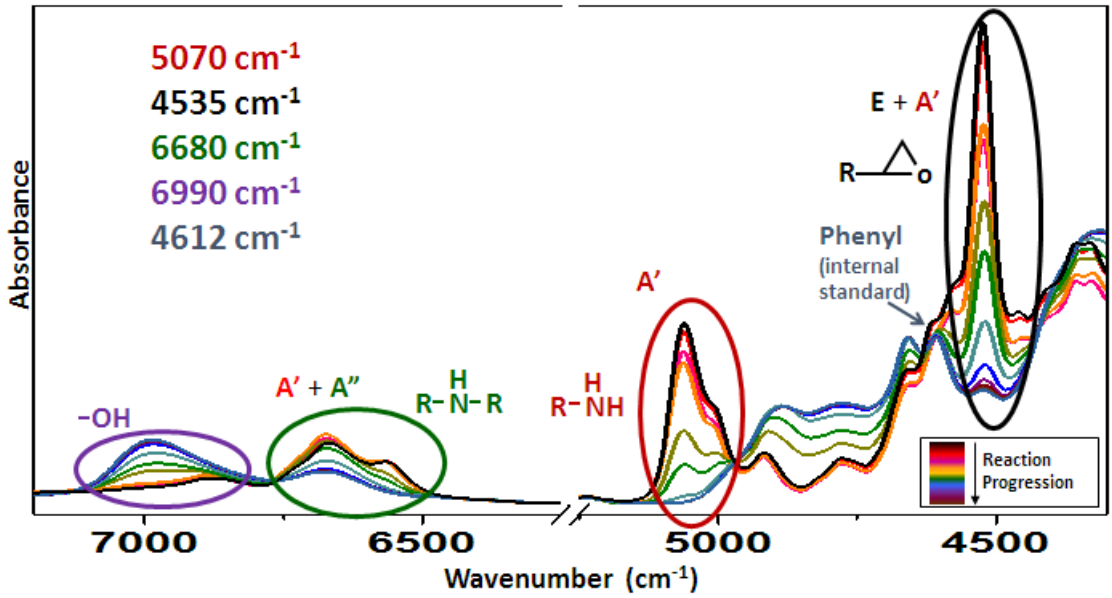

Figure 3.5 Series of stacked spectra of T-33 taken throughout cure with the peaks of interest identified.

It is often stated in literature that the absorption coefficient (ε) is a constant. This term is then used to calculate chemical group concentration at an IR band of interest using Beer's Law as in Equation 1.3.[70] The analysis of absorbance signals are typically normalized to an internal standard peak representing a nonreactive species in order to account for subtle changes in path length, sample viscosity, and refractive index. This adjustment simplifies the Beer's Law equation and directly relates absorbance to functional group concentration (*c*) and the path length normalized molar absorptivity term (*a*). Molar absorptivity can more accurately be described as a constant for a functional group at the IR band for conditions in which it is measured and is therefore not a true constant. It has been reported in the literature that molar absorptivity changes as a function of temperature, however the effect has been viewed to be not unlike the changes which occur via path length.[87] Thus, a constant molar absorptivity value is traditionally still used in the analysis of functional group concentration during cure. It has been

determined in this work, however, that it is incorrect to discount the temperature effect on molar absorptivity because the change to the absorbance signal is not uniform across the spectrum. This will be discussed in greater detail below.

Ignoring changes in absorptivity has previously been acceptable because IR studies of epoxy cures would be performed by removing aliquots from a separate curing vessel and acquiring IR scans of the sample at discreet time points at a single temperature (e.g. room temperature). Real time NIR obtains scans of the reacting network during cure, however it also means data acquisition occurs at different temperatures. Studies comparing systems cured with matching temperature profiles may not require a correction as any change in temperature over time is the same for all systems. Noting this effect is important for this study, because the samples are subjected different temperatures at different times throughout cure.

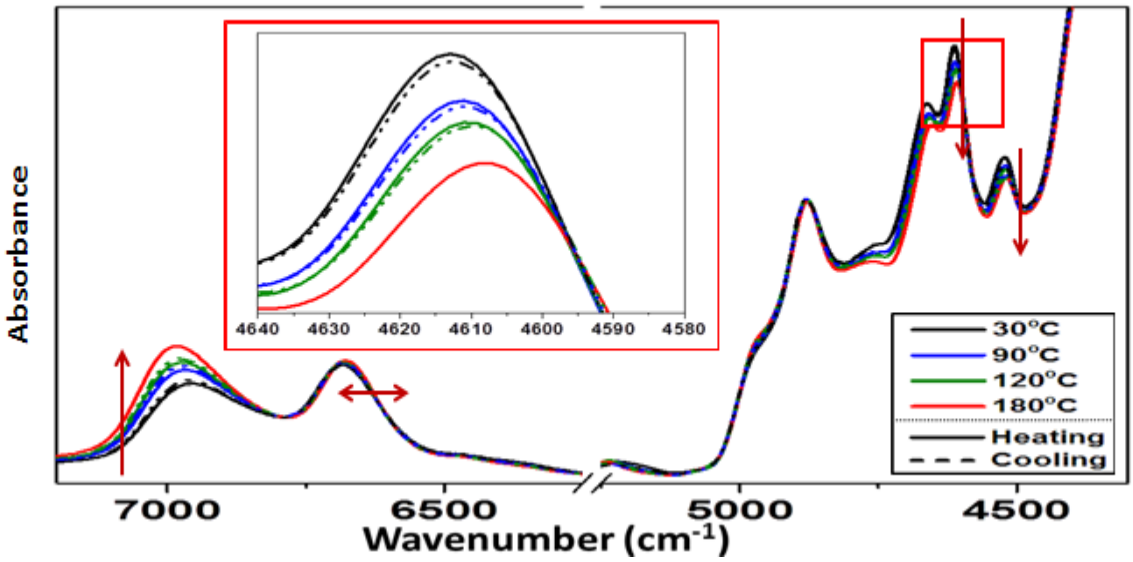

Figure 3.6 Spectra of a cured sample collected during one heat/cool cycle. Inset shows change in absorbance area of the nonreactive aromatic peak. Arrows indicate the trend of peak area for the given peak when heated.

To ascertain the temperature effect on absorbance, a cured sample of T-44 was heated from room temperature to 180 °C then cooled to its initial temperature. Figure 3.6 confirms that absorbance is affected by temperature but not uniformly across the spectrum, indicating frequency specific temperature effects on absorbance. The sample is not undergoing significant reaction; therefore, these changes are due to changes in molar absorptivity. The peak representative of the nonreactive aromatic groups, monitored through several heat/cool cycles (Figure 3.7), displays a repeatable and predictable temperature effect on molar absorptivity. Because the concentration of aromatic rings in the system is a known constant it was possible to calculate the change in absorptivity with temperature. The data shows that the peak area decreases 0.35% for every degree above 30 °C, which was used as the reference temperature.

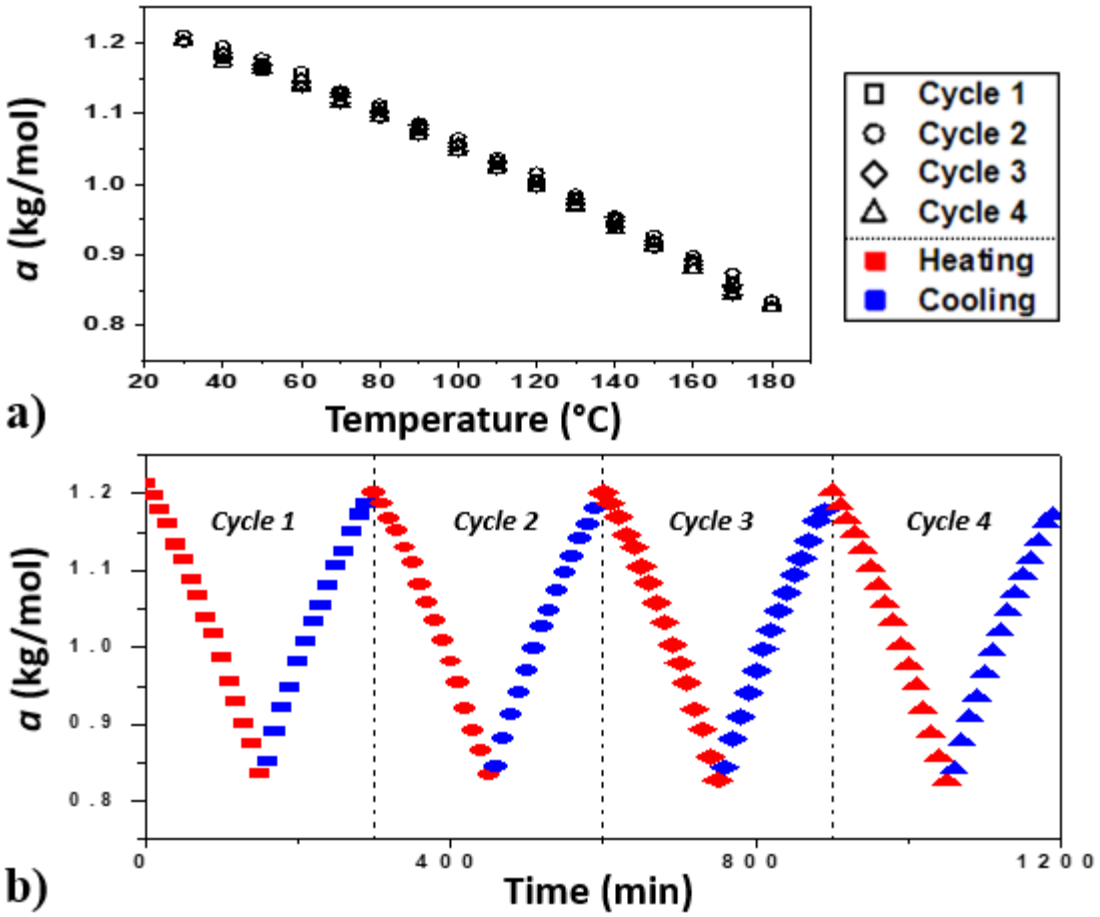

Figure 3.7 Molar absorptivity of the aromatic peak cycled from 30°C to 180°C four times.

Further investigation into the change in absorbance of the relevant peaks in the cure of epoxy/diamine networks is shown in Figure 3.8. Here a T-33 network was used to study the change in absorbance with temperature. It is clear these peaks have repeatable and predictable changes in absorbance as a function of temperature. The changes in absorbance are plotted normalized to the absorbance at 30 °C, which was the reference temperature from which an initial value of molar absorptivity calculated. This was achieved by using a known initial functional group concentration at the beginning of cure, as is traditionally done in Beer's Law calculations. In this work the change in absorptivity with temperature was determined by using heating and cooling cycles for a

previously cured network. This was done to insure constant concentrations of the functional groups studied throughout thermal cycling and to eliminate absorbance complexities which arise from changes in physical state during the collection of IR spectra. However, this approach prevented the determination of the temperature dependence of the molar absorptivity of primary amines, which were fully consumed in the tested samples. Table 3.1 lists the molar absorptivity (a_{ref}) determined for key functional calculated at 30 °C for the epoxy/diamine cure as well as the fractional change in absorptivity per degree (a_{cf}) from the 30 °C reference value.

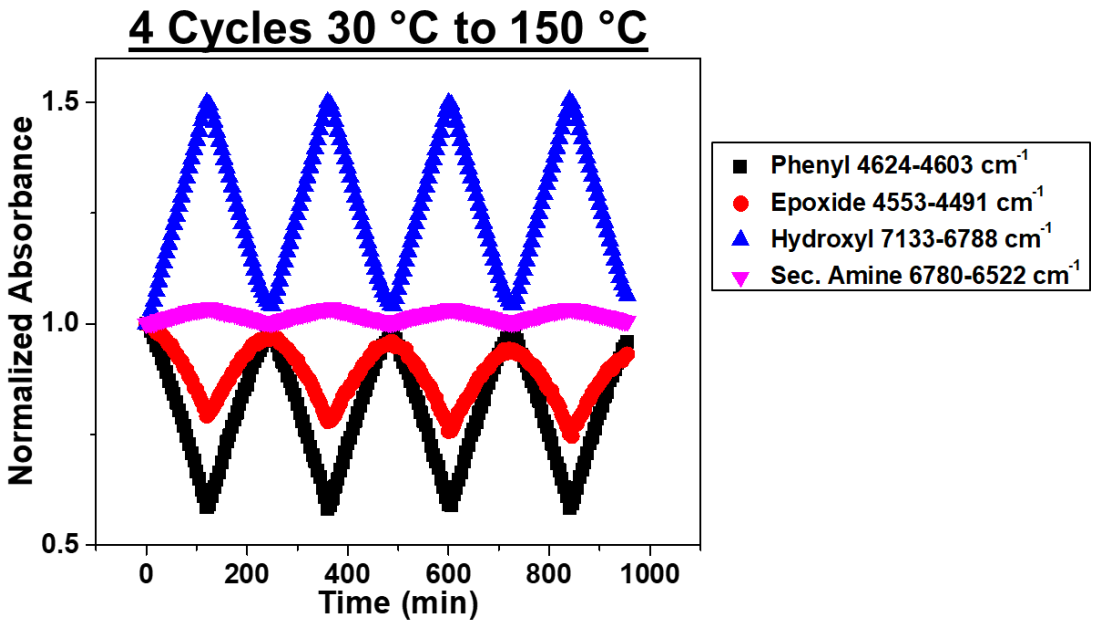

Figure 3.8 Change in the absorbance of the four peaks of interest available in a postcured sample upon four heat/cool cycles from 30 °C to 150 °C.

Table 3.1 Molar Absorptivity and the Fractional Change Per Degree

Functional Group	Wavenumber Range (cm^{-1})	Molar Absorptivity at 30 °C (a_i)	Fractional Change in Absorptivity per Degree (a_c)
Epoxide	4553-4491	3.081	-0.00172
Primary Amine	4553-4491	0.3912	-
Aromatic	4624-4603	1.212	-0.00350
Primary Amine	5112-5044	3.872	-
Primary Amine	6780-6522	6.586	-
Secondary Amine	6780-6522	10.11	0.0004047

The change in absorbance is not related to a change in path length as verified using Thermomechanical Analysis (TMA) data. Figure 3.9 shows a slight linear thermal expansion for a cured RT-NIR sample cell. The observed increase of 0.0113% per above 30 °C does not match the trends observed for the changes in molar absorptivity with increasing temperature. Additionally, the increase and decrease in the absorbance signals for different functional groups with increasing temperature further illustrates that unlike thermal expansion (which would increase absorbance across the whole spectrum) changes in absorptivity must be individually corrected for in the analysis of each functional group.

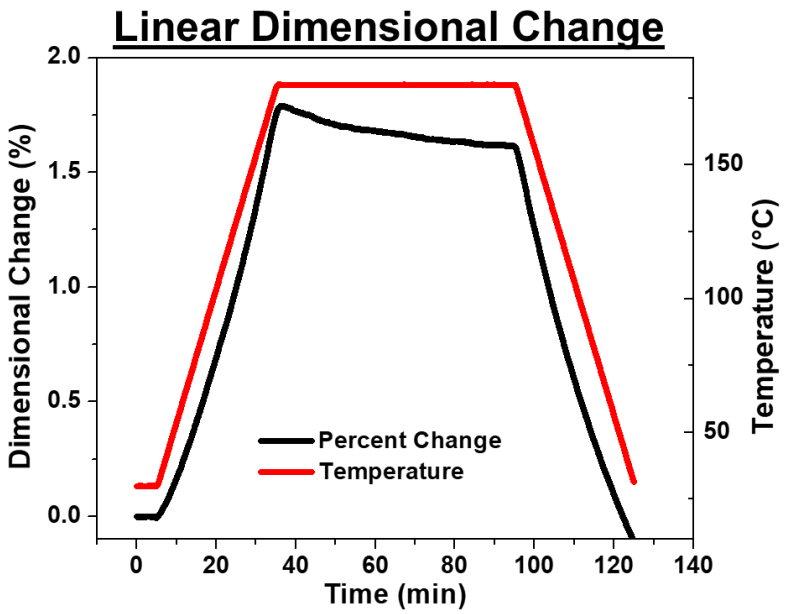

Figure 3.9 Dimensional change over a 5 °C/min temperature ramp from 30 °C to 180 °C followed by a 1-hour isotherm and 5 °C/min cool to room temperature.

$$A_c = \frac{c_i a_{ref}}{(1+(T_i - T_{ref})a_{cf})} \quad \text{[Equation 3.1]}$$

Based on the data, a temperature correction factor was formulated to account for the change of molar absorptivity with temperature and correct the absorbance in order to accurately calculate functional group concentration (Equation 3.1). Here A_c is the corrected absorbance value, a_{ref} is the initial molar absorptivity determined at the reference temperature, and a_{cf} is the fractional change per degree of the absorptivity due to temperature. This correction factor was used to adjust *in situ* cure spectral data.

Epoxide conversion determined via this improved RT-NIR analysis was compared degree of cure data taken from DSC. The integration over time of the cure exotherm for identical networks cured with different protocols show a high degree of agreement with the calculated epoxide conversion, which lends confidence to the necessity for the temperature correction (Figures 3.10 and 3.11). It should be noted that

over the course of the 180 °C isotherm all the samples achieve the same degree of conversion regardless of ramp rate; DGEBF based systems reached 100% conversion, while the higher crosslinked TGDDM system achieved ~96 % conversion for all protocols. This will be discussed in greater detail in Chapter IV.

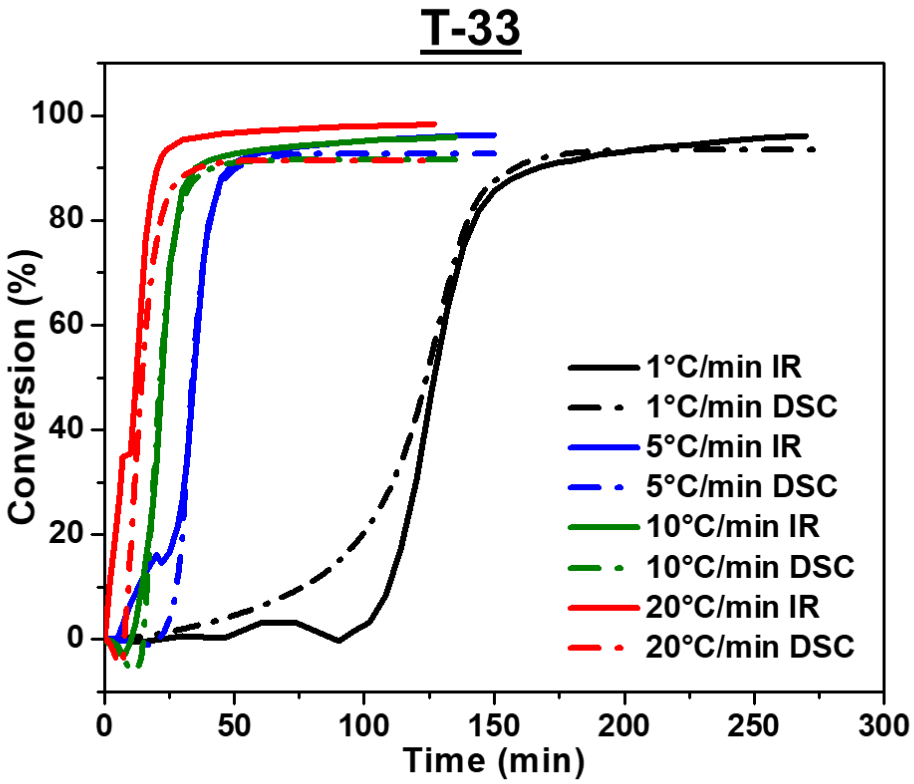

Figure 3.10 T-33 epoxide conversion vs DOC as calculated from DSC.

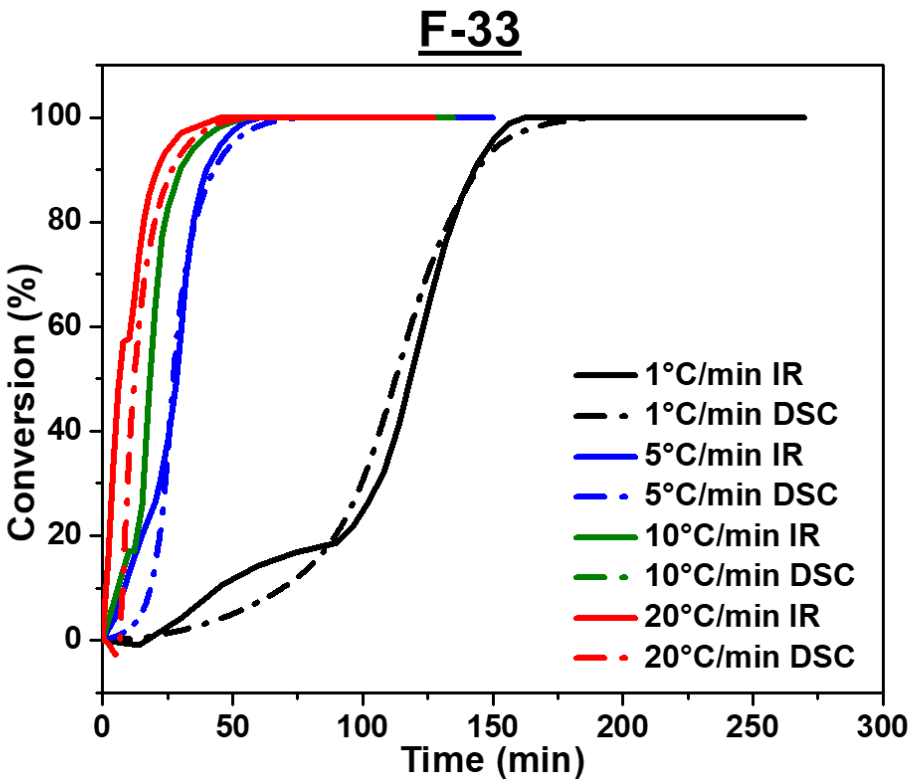

Figure 3.11 F-33 epoxide conversion vs DOC as calculated from DSC.

Further validation was performed using a F-33 system reacted to a point pre-gelation. Here, the F-33 sample was ramped at 5 °C/min for 29 minutes then removed from the heat cell and quenched to stop the reaction (Figure 3.11). The conversion of epoxide and primary amine groups by RT-NIR analysis was 28.8% and 50.0% respectively. The quenched epoxy/amine system was then recovered from the RT-NIR sample cell and analyzed for degree of cure in DSC. The reduction of primary amine proton signal was analyzed by NMR spectroscopy to verify the RT-NIR concentration results. The integration for the peak representative of the primary amine protons at 5.2 ppm was normalized to the signal of the protons on the aromatic peak. A reduction in peak intensity of nearly 50% as well as the appearance of a peak representative of secondary amine protons at 5.6 ppm was observed. As indicated by Figures 3.13 and

3.14, the data are in excellent agreement, confirming the validity of the correction factor applied to molar absorptivity.

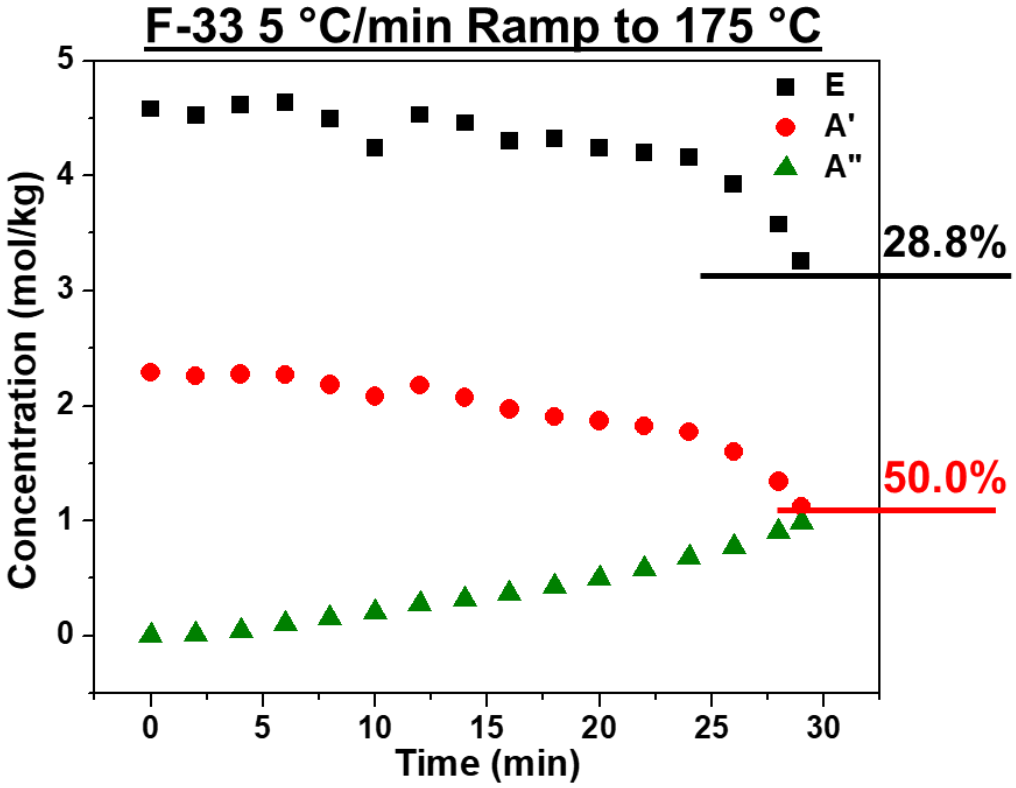

Figure 3.12 Concentration vs. Time graph of F-33 system ramped from 30 °C to 175 °C at a rate of 5 °C/min indicating the calculated conversion of epoxides (E), primary amines (A'), and secondary amines (A") at the point the reaction was halted.

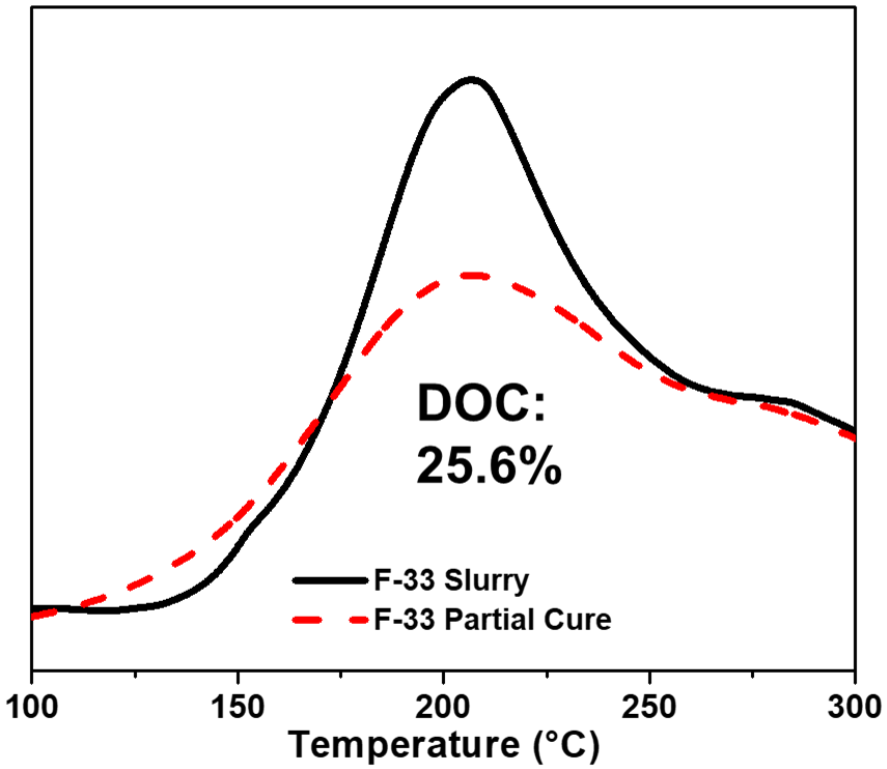

Figure 3.13 ΔHUC and ΔHC of a F-33 slurry before reaction and after partial cure in the RT-FTIR cell.

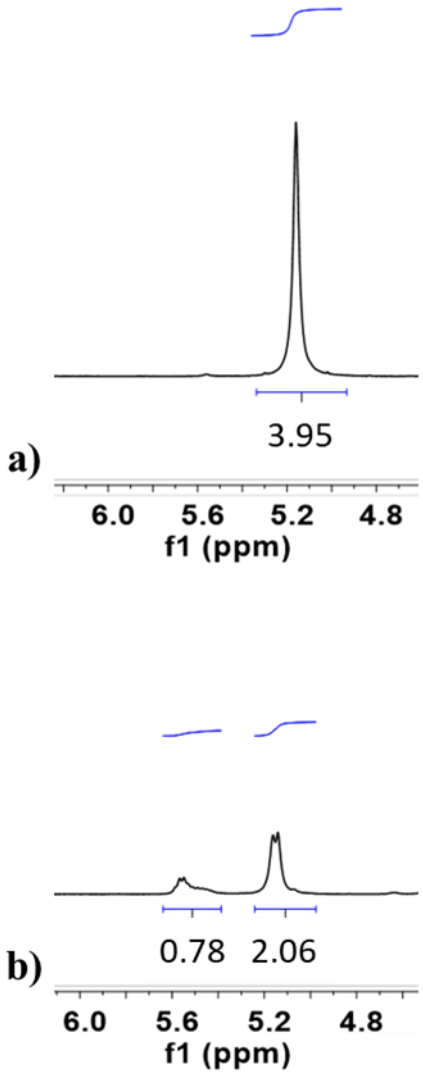

Figure 3.14 Proton NMR spectra of F-33: a) initial slurry; b) after reaction to a point prior to gelation in the RT-NIR cell.

3.4 Conclusions

The calculation of functional group conversion via Beer's Law has been refined by identifying the temperature effect on molar absorptivity, which must be accounted for when attempting to analyze network formation during a nonisothermal cure. A correction factor for the absorptivity of functional groups at elevated temperatures was implemented. This proved to significantly improve the reliability of molar concentration

data needed to accurately study the pathway of network formation. A high degree of agreement was observed between the RT-NIR data and traditional DSC methods using this correction factor. This validates using RT-NIR spectroscopy to monitor cure kinetics.

CHAPTER IV – EPOXY/DIAMINE NETWORK FORMATION MONITORED IN REAL TIME VIA FTIR

4.1 Chapter Overview

The effects of rapid cure rates on the formation of epoxy/diamine glassy thermoset networks such as those commonly used as matrices in high performance composite panels are yet to be determined. While there are many potential effects to consider when decreasing matrix cure cycle time, this work seeks to understand the effect of varied cure protocols on epoxy-amine network formation during cure. Traditionally, much attention is placed on the final material properties of a cured network and this becomes the only metric to determine the effect of some experimental variable, such as cure protocol. Very little is understood about the state of the network during cure, as the network develops. This is predominantly due to the limited availability to quantify the extent of the epoxy/amine reaction with traditional characterization techniques such as rheology and dynamic scanning calorimetry (DSC).

This work showcases the ability to directly monitor the development of epoxy/diamine networks using real-time Fourier transform infrared spectroscopy (RT-FTIR). With this technique the concentration of specific functional groups can be observed independently throughout cure. This contrasts with the more commonly used DSC heat of reaction technique, which produces one degree of cure value for analysis. RT-FTIR is not only able to quantify the extent of reaction but is also able to distinguish the identity of functional groups reacting. As demonstrated in Chapter III the quantifiability of this technique has been affirmed and therefore the information gained with regard to relative concentration of reactive groups have a high degree of validity.

Monitoring the concentration of reactive functional groups in curing epoxy/diamine systems is a key factor towards understanding the pathway of network formation An understanding of the pathway of network formation by this analytical method also has the potential to inform and improve predictive computer modelling.[88]

For this chapter, three networks were studied. The potential role of the structural isomerism of two common amine curative has on network formation was investigated by comparing T-33 to T-44 networks. The cure of F-33 networks was also compared to T-33. DGEBF is difunctional and therefore would tend toward linear growth prior to crosslinking if all primary amine reacts prior to the formed secondary amine. The overall lower average functionality of the F-33 means that a higher percentage of the total reactions will need to occur before the system gels and reaches infinite molecular weight.

4.2 Network Formation Pathway as a Function of Thermal Ramp Rate

For this chapter, RT-NIR is the primary tool used to monitor network growth though cure. The effect of the cure protocol on matrix formation was studied by maintaining several consistent variables. The beginning temperature as well as the temperature of the isotherm were kept consistent (30 °C and 180 °C respectively). The dwell (length of time) of the isotherm applied to a full cure protocol was also kept consistent at 2 hours for all networks and cure protocols. The chemical structures of the network components studied and the thermal ramp rate to the isotherm were the only variables changed.

Figures 4.1, 4.2, and 4.3 contain many graphs that monitor the concentration of a functional group in the curing system. The logged concentrations are of the epoxide group (E on the graphs), primary amine (A’), and secondary amine (A”). The units of

concentration, it should be understood, are mols per kg, and refer the mols of the functional group in the system. The initial concentration of epoxides and primary amines in the slurries is directly calculated from the molecular weight of the monomers and their functionality. The average functionality of the T-33 and T-44 systems are the same and the molecular weight of the DDS monomers, of course, equal. The initial molar concentration of epoxides in the TGDDM based formulations is 5.963 $mol.kg^{-1}$. The initial concentration of primary amines is 2.981 $mol.kg^{-1}$. For the F-33 system the initial concentration of epoxides in 4.582 $mol.kg^{-1}$ and 2.291 $mol.kg^{-1}$.

It is important to note that by the nature of the epoxide/diamine reaction the theoretical maximum concentration of secondary amines during cure and network growth equals the initial concentration of primary amines. This would only happen in the case where all primary amines react (creating secondary amine) prior to any secondary amine reacting into the system. When interpreting concentration vs. time graphs for epoxy/diamine cures special attention should be payed to the peak height of the secondary amine curve, because it will indicate how much free secondary amine was created without reacting into the network. This is one of the main ways to determine the pathway of growth for an epoxy/diamine network.

In the below figures, it can be observed that over the course of the isotherm at 180 °C all the samples reach approximately the same conversion (i.e. the final concentration of epoxide groups) for each formulation regardless of ramp rate. DGEBF based systems all reached 100% conversion while the higher crosslinked TGDDM systems reach epoxide conversions of ~96 % and ~91% for T-33 and T-44 networks respectively.

In comparing the TGDDM based systems (Figures 4.1 and 4.2), primary amine (A') is consumed at a faster rate with increasing ramp rate, and it is interesting to note that at all ramp rates, the onset of the reduction of secondary amine concentration (A") occurs prior to A' exhaustion. At each ramp rate the time at which primary amine is exhausted is closely followed by the conversion plateau of epoxide. For both systems, and at all ramp rates, when primary amine reaches 100% conversion epoxide conversion has already greatly exceed 50%. This indicates that both epoxy/diamine networks do not undergo linear growth followed by crosslinking, but rather that crosslinking occurs concurrently with molecular weight increase.

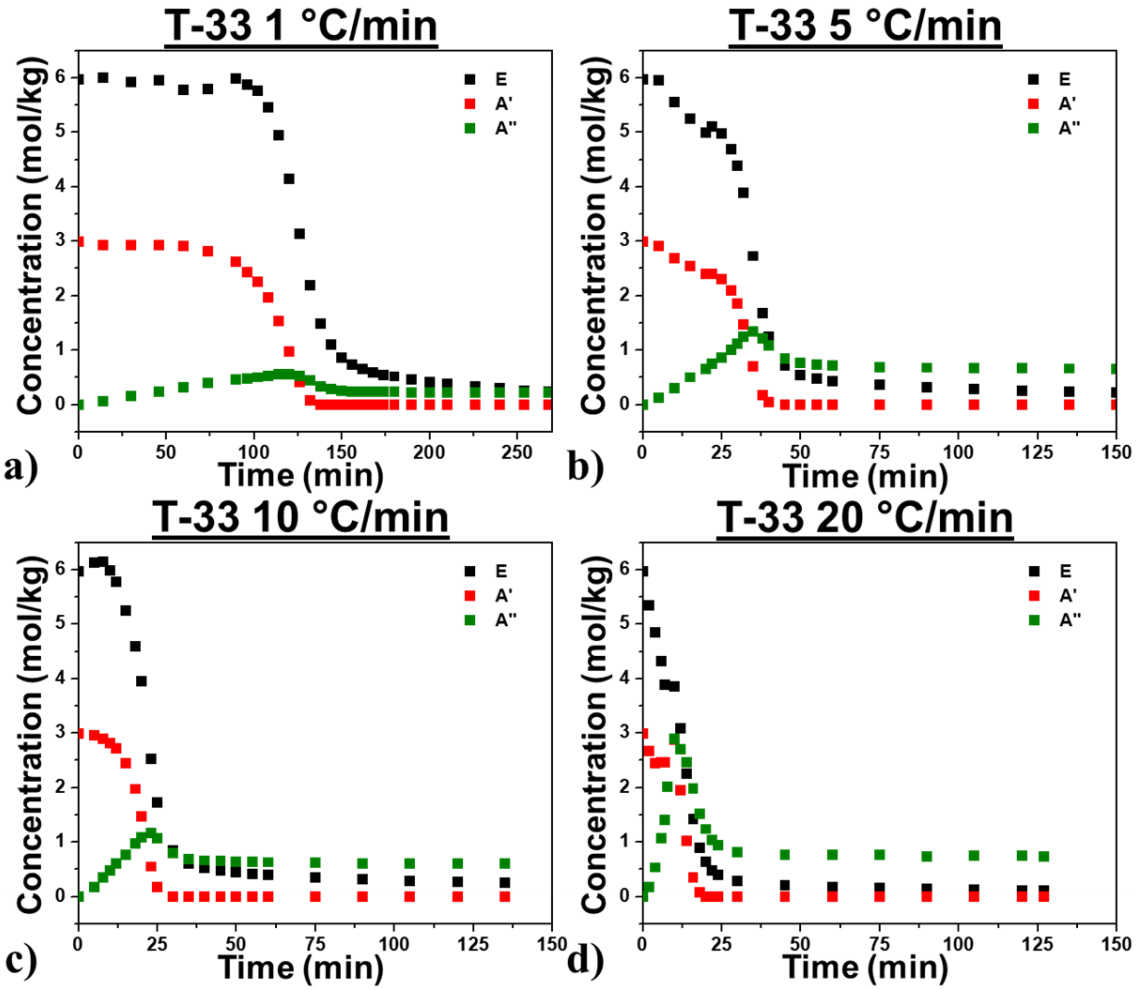

Figure 4.1 T-33 concentration vs. time graphs for epoxide (E), primary amine (A'), and secondary amine (A") functional groups for four cure ramp rates.

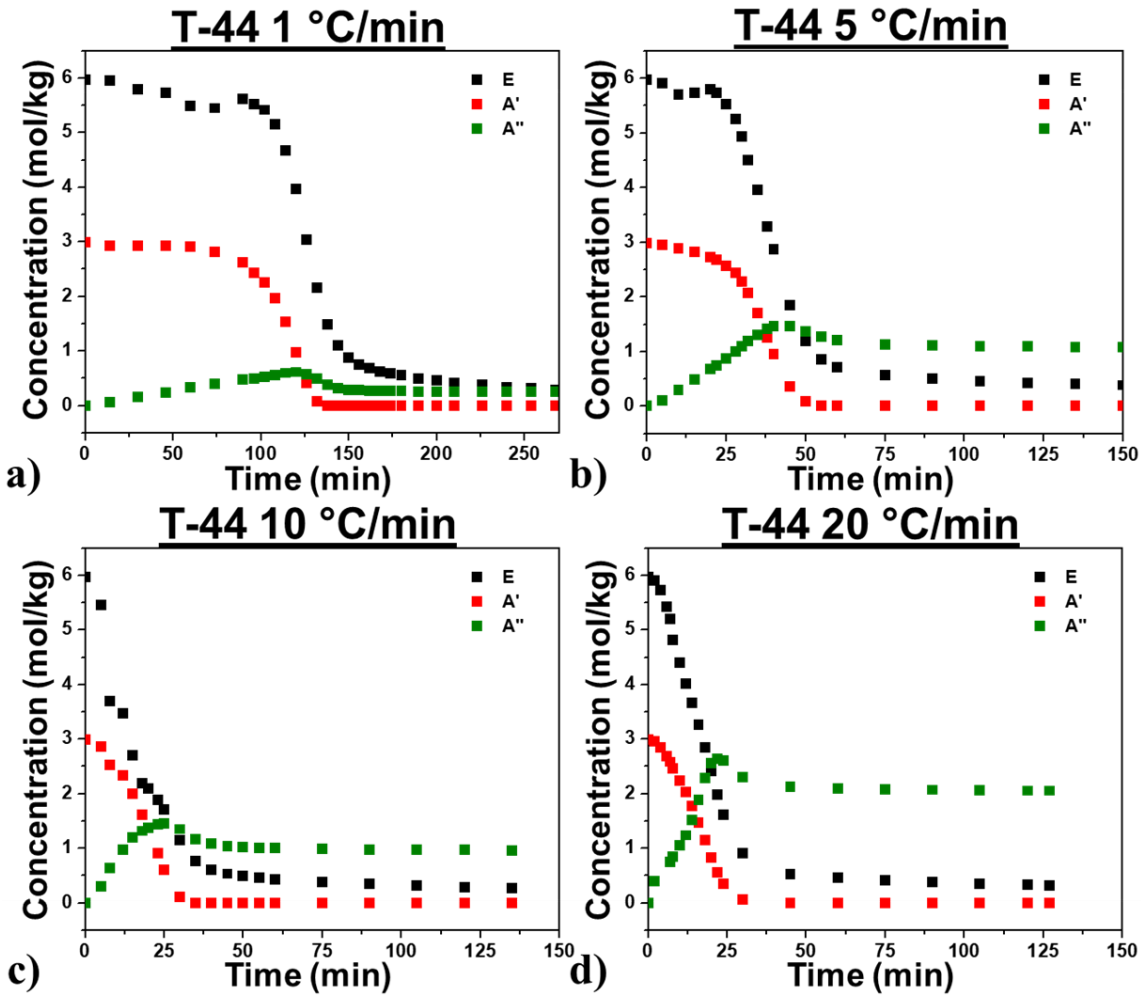

Figure 4.2 T-44 concentration vs. time graphs for epoxide (E), primary amine (A'), and secondary amine (A") functional groups for four cure ramp rates.

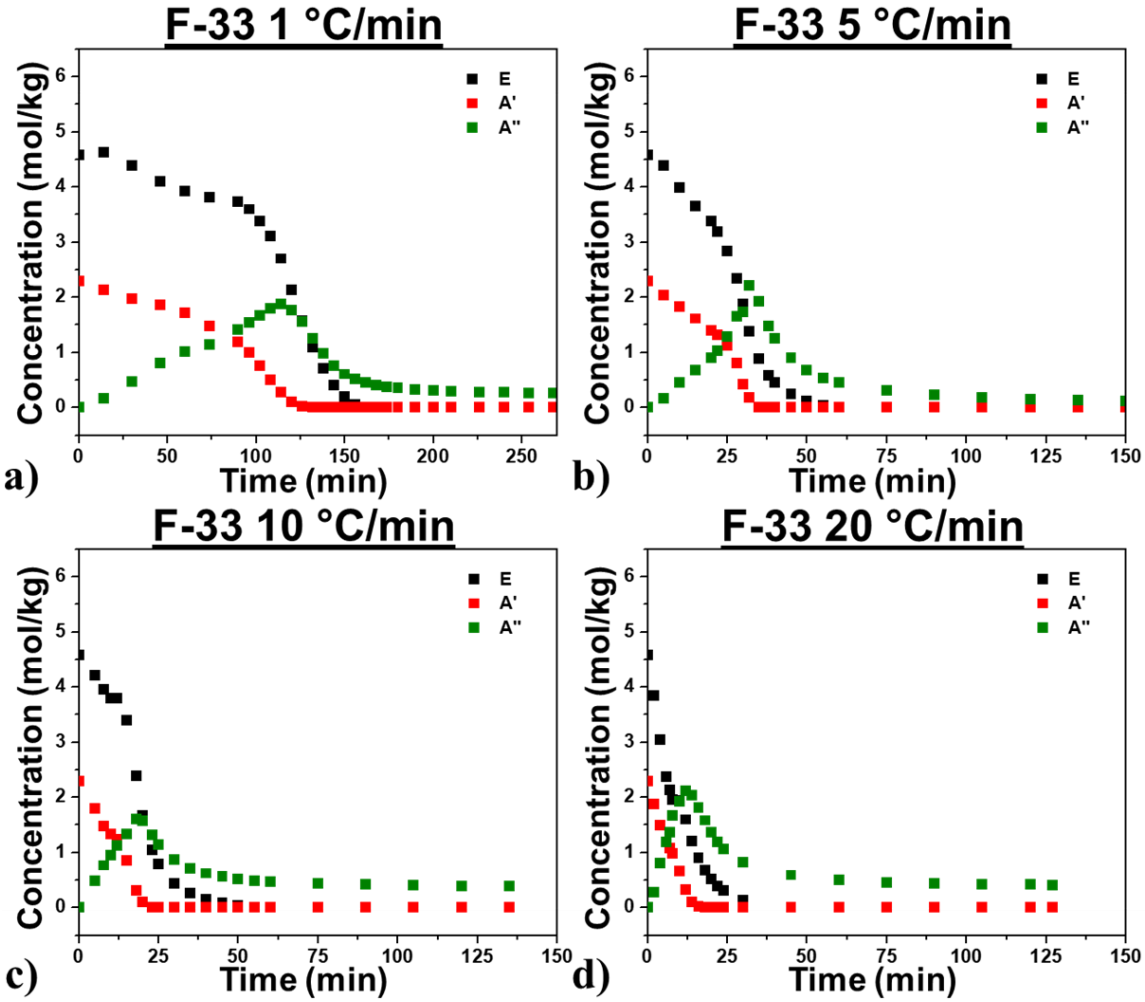

Figure 4.3 F-33 concentration vs. time graphs for epoxide (E), primary amine (A'), and secondary amine (A") functional groups for four cure ramp rates.

The most information can be gained on network formation pathway by observing the shape of secondary amine concentration curves (Figures 4.4, 4.5 and 4.6). The trends in peak height and the eventual plateaus are different for each network as a function of cure protocol. It is easier to understand the differences in the developing network architectures by analyzing the networks in two groups. By comparing T-33 to T-44 the role of the structural isomer of DDS can be determined and the role of average functionality can be discerned when comparing F-33 to T-33.

For both TGDDM systems a cure protocol dependence is observed. The fastest ramp to the isotherm leads to a secondary amine peak closest to the maximum of any of the cure protocols. Also, the slowest cure path produces a curve with the lowest peak. It is worth emphasizing here that a lower peak does not mean less reaction occurred as might be the case if primary amines did not react to produce a higher concentration of secondary amine. It is known that all the primary amines react in these cures and that the epoxides reach high conversion, so secondary amine is present and reacting during cure. The molar concentration of secondary amines is best looked at as a net value. When secondary amines are consumed as they are created the observed concentration will remain low. In both T-33 and T-44 there is a trend of faster ramp leading to the preferential consumption of primary amine prior to the consumption of secondary amine.

The other major characteristic of the secondary amine molar concentration curve which should be analyzed is the point where consumption of the amine stops, resulting in a concentration plateau. In both TGDDM based networks, regardless of thermal ramp rate, the total amount of epoxide converted was approximately equal. However, it can be clearly seen that for the more rapidly cured systems the concentration at which secondary amine consumption plateaus increases. The formulations of all of the networks studied were prepared with equal amounts of epoxides and amine active hydrogens. The high plateau observed in the rapid cure of T-33 and T-44 suggest a large portion of epoxide is being consumed by a means other than the amine reaction. The most likely alternative is the etherification reaction. The potential to monitor the etherification in epoxy/diamine cures will be discussed in further detail later.

The concentration of the secondary amine plateau in the T-44 networks is higher than those of all the T-33 networks with analogous cure ramp rates. Two potential reasons for this difference are that the T-44 network cures slower than T-33 and the 44DDS monomer is more rigid. This may lead to a network which forms in such a manner as to not allow for secondary amine to diffuse to and react with available epoxides.

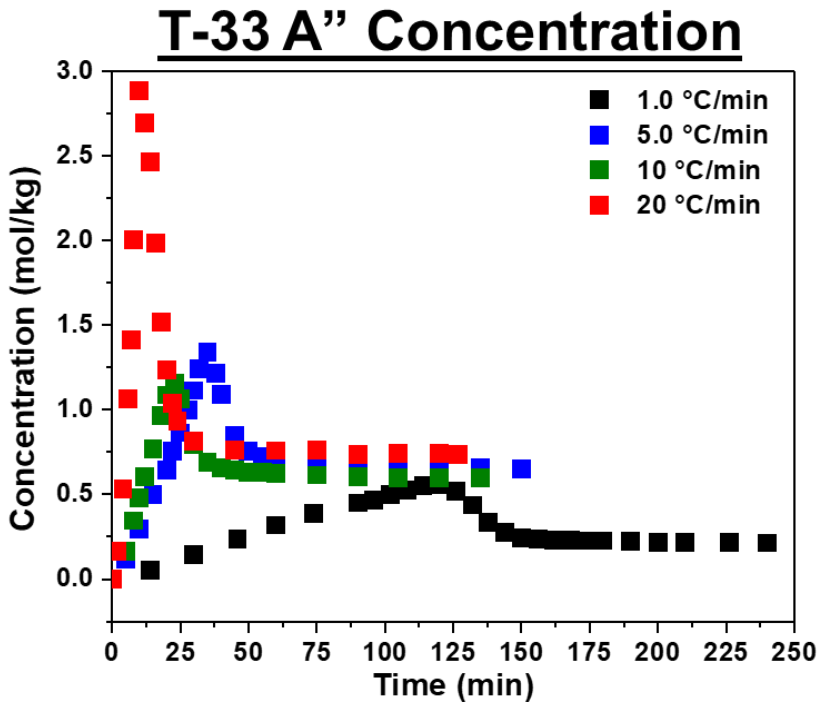

Figure 4.4 Concentration of secondary amine versus time of T-33 networks cured with thermal ramp rates of 1, 5. 10, and 20 °C/min.

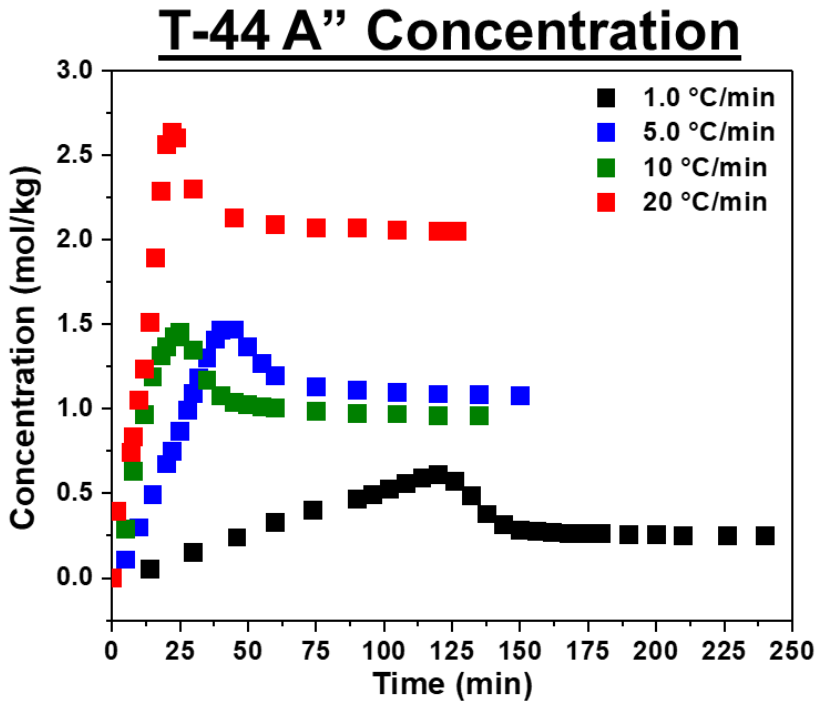

Figure 4.5 Concentration of secondary amine versus time of T-44 networks cured with thermal ramp rates of 1, 5. 10, and 20 °C/min.

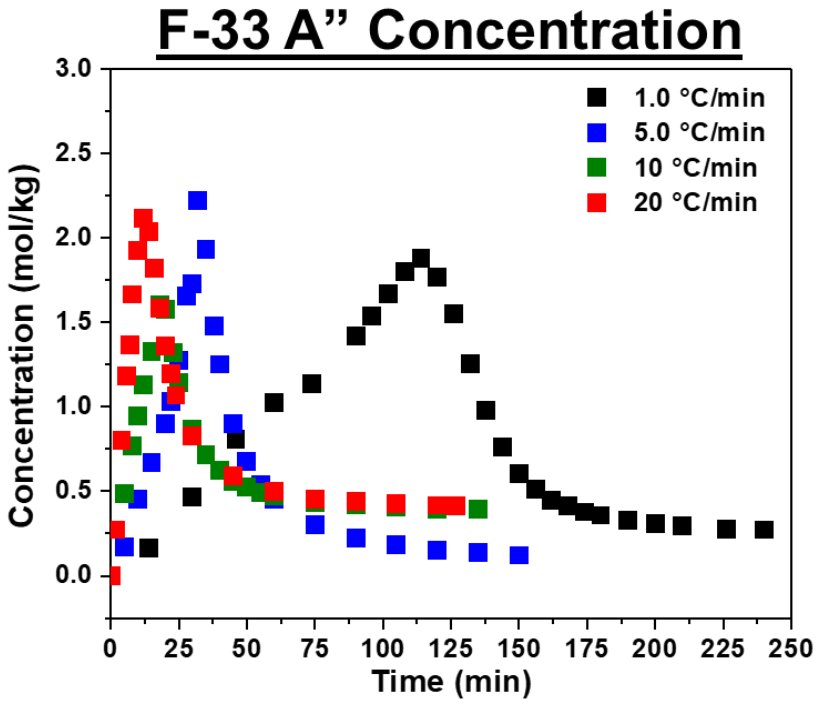

Figure 4.6 Concentration of secondary amine versus time of F-33 networks cured with thermal ramp rates of 1, 5. 10, and 20 °C/min.

Comparing the difunctional based epoxide F-33 to T-33 reveals a dramatically different response of the two systems to varied ramp rates. The relatively consistent peak concentration of A” in the F-33 systems indicates a similar network growth pathway independent of cure ramp rate. The T-44 networks display a dramatic effect of the ramp rate. The lower maximum of A” concentration observed in the slower cure protocols is not indicative of any undercure relative to the faster cured networks, as indicated by the equivalent final conversion. The lower peak indicates a greater abundance of tertiary amine present in the system earlier in network formation for these slower cured networks. This would result in localized areas of higher crosslink density in the early stage of cure for these systems. The consequence of this different network growth pathway merits further investigation into the effect on final network mechanical properties of networks cured with using these increasing ramp rates. The faster cures (10 and 20 °C/min) of F-33 also exhibit a secondary amine concertation plateau higher than that of the slower cure protocols.

4.3 Evidence of Etherification

There is compelling evidence to suggest that etherification reactions are occurring in the epoxy/diamine networks studied in this work. Historically, the contribution of the etherification reaction has been deemed to not be a major factor in network development. It was believed that significant etherification can only happen at high temperatures held for extended times. The data collected in this work proves the etherification reaction occurs in these high T_g epoxy/diamine systems at temperatures much lower than previously identified.

Figure 4.7 shows the change in absorbance for the aromatic, epoxide, and hydroxyl peaks of a cured T-33 network over ten heat-cool cycles from 30 °C to 150 °C heated and cooled at a rate of 1 °C/min, normalized to the absorbance at 30 °C. Frequency specific temperature effects on the absorbance of these signals can be observed for all three peaks which agree with the findings reported in Chapter III. The aromatic signal maintains the change in slope and consistency previously observed. The hydroxyl peak is also consistent, always returning predictably. The epoxide peak shows a slow reduction in peak signal at 30 °C. This indicates consumption of epoxide during the cycling. However, the unchanging nature of the hydroxyl peak suggests that the epoxides may be undergoing an etherification reaction rather than reacting with amine, as an epoxide/amine reaction results in the production of a hydroxyl group. Figure 4.8 shows the change in absorbance of the functional groups monitored and also does not show a reduction in the epoxide peak absorbance when samples was only raised to 100 °C (well below the point of any expected post-curing) indicates that reaction is occurring during this cycling to higher temperatures.

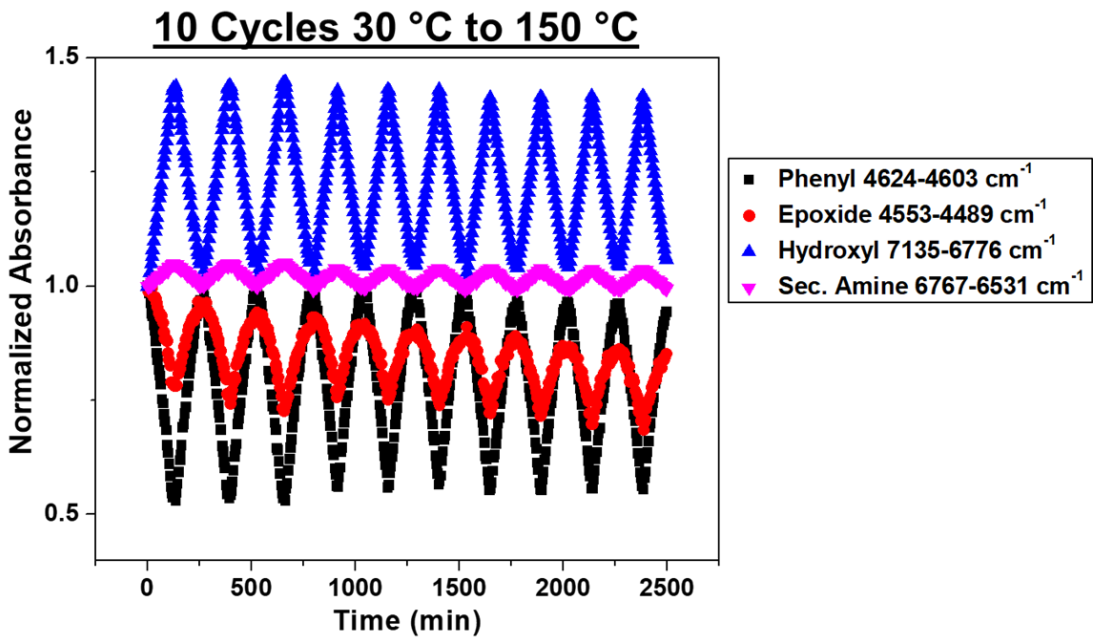

Figure 4.7 Change in normalized absorbance over 10 heat/cool cycles from 30 °C to 150 °C for the available peaks of interest.

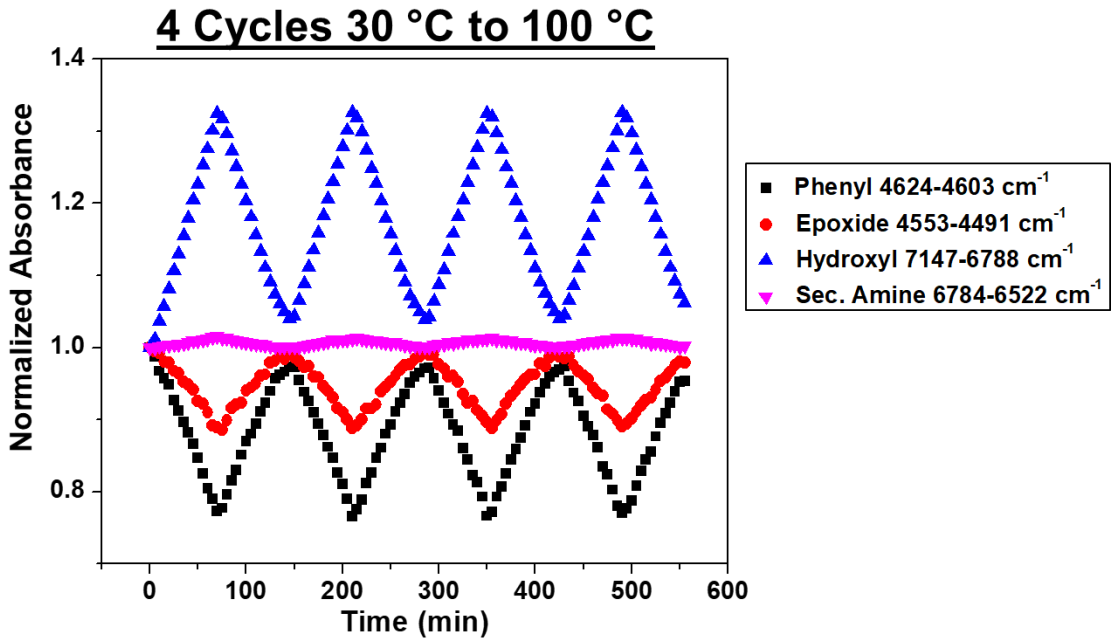

Figure 4.8 Change in normalized absorbance over 4 heat/cool cycles from 30 °C to 100 °C for the available peaks of interest.

Further evidence of etherification can be observed in Figure 4.9. A pre-cured T-33 network was held at three different isotherms for 3 hours. The large offset in epoxide

conversion does not match up with the growth in hydroxyl peak that would represent the formation of an epoxy-amine linkage. Etherification of epoxide reacting with hydroxyl creates another hydroxyl group so the net result is no change in concentration. The trends observed strongly indicate this is what is happening during the post cure rather than further reaction with available secondary amines. It is worth pointing out that the etherification observed in cured network is taking place below the T_g of the network and is therefore occurring in a state of limited mobility. This analysis may further be expanded to quantify etherification reactions during cure.

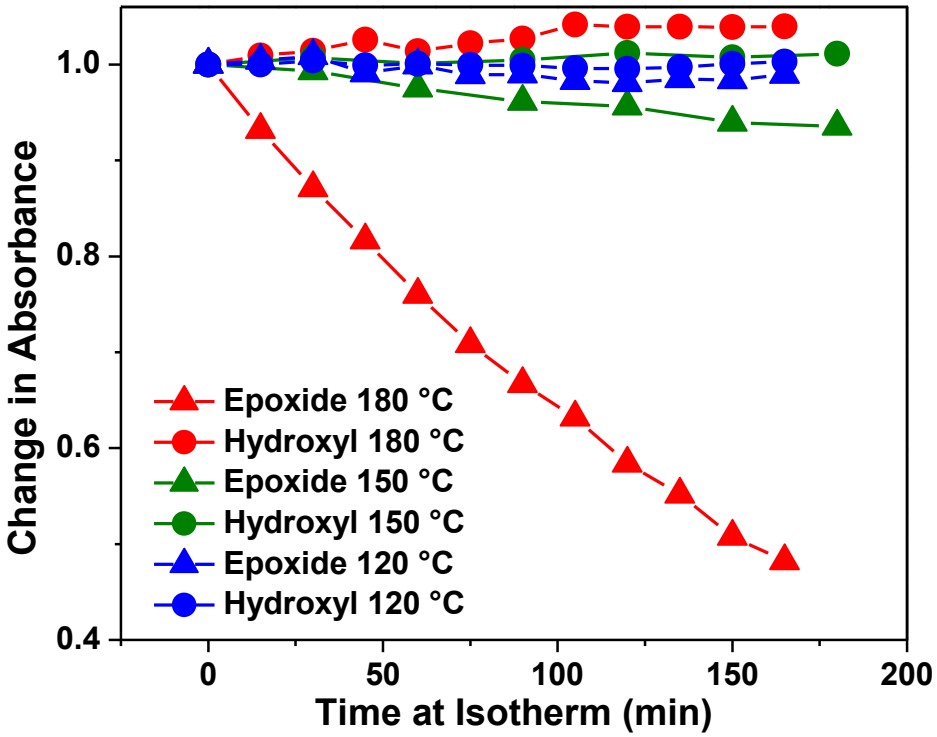

Figure 4.9 Percent change in absorbance of epoxide and hydroxyl peak of already cured sample during isothermal post cure at 180 °C, 150 °C, and 120 °C.

4.4 Conclusions

In this work, it was proven that irrespective of ramp rate for all of the TGDDM based networks primary and secondary amine react concurrently, and crosslinking occurs at early stages of network growth. However, differences are observed in both networks in the timing and rate of secondary amine production and consumption. This indicates differences in the relative dispersion of crosslink density during different points for cure for networks cured using different cure protocols. The TGDDM based networks show that when cured with a slower ramp rate the secondary amine reacts to a great extent while primary amine is still available to react. This indicates the formation of localized areas of high crosslinking as tertiary amine linkages are created an a “micro gel” like growth pathway is taken. The faster cures however, in all the systems studied exhibit higher plateaus of secondary amine concertation at the end of cure which means that secondary amine does not appreciable continue to react. In many of these cases the concentration of epoxide continues to be reduced. Etherification is believed to be the leading reaction in this region. The role presence of etherification reactions in already formed networks was identified at temperatures well below the glass transition. The development of RT-NIR to monitor network growth of thermosets has the potential to improve the understanding of cure pathways.

CHAPTER V – EFFECT OF CURE PROTOCOL ON EPOXY/DIAMINE NETWORK MATERIAL PROPERITES

5.1 Chapter Overview

Increased temperature ramp rate for curing thermoset polymer networks is desirable for reducing manufacturing cycle time, especially as novel out-of-autoclave technologies continue to drive the industry standards. There are many factors to consider when increasing processing temperature ramp rates; this project's goal was to understand changes or differences in epoxy/diamine network properties as a function of cure protocol. Initially, TGDDM was selected as a standard multi-functional epoxide prepolymer in order to facilitate comparison with commercial formulations. 33DDS and 44DDS are also common aerospace matrix curatives which allow for an investigation into isomer effects on network formation. Selection of these two curatives allows for consistency in the chemical and physical compositions of the networks, such as molecular structure and molecular weight between crosslinks. However, curing networks with the para-substituted 44DDS or meta-substituted 33DDS affects the reactivity of curative in the formulation as well as the conformational freedom of the curative during network formation. These two factors were determined to affect the network formation pathway of T-33 and T-44 when cured with different thermal protocols as determined by RT-NIR analysis and the effect of those altered pathways on macroscopic material properties was investigated.

Later, in the course of this work, the role of epoxide prepolymer functionality was investigated. Networks cured with the tetrafunctional TGDDM were compared to analogous formulations cured with DGEBF, which has a similar backbone structure but is

difunctional. These epoxide prepolymers were both cured with 33DDS in order to keep the diamine constant and directly probe the role of average functionality of epoxide/diamine systems cured with different thermal protocols. The lower average functionality of the F-33 system was expected to alter the gelation behavior of the network as more conversion is required to take place before a continuous network is formed. DGEBF also has a lower room temperature viscosity that TGDDM. The role of the viscosity of the curing systems up to the point of gelation was also studied.

5.2 Traditional versus Slurry Preparation Method

The main goal of this project was to study the cure pathway for epoxide/amine reactions and how that may be affected by different cure protocols such as the temperature ramp rate to isotherm. One of the main network properties of interest was DOC along with the evolution of properties during cure as the network developed. It was hypothesized that the *traditional* method of materials preparation may initiate reaction. To accurately relate DOC to sample properties, all samples must begin at zero conversion. This concern led to the decision to investigate the utility of using slurries homogenized by a speed mixer as described in Chapter II.

Heat of reaction experiments on TGDDM/DDS mixtures were performed using DSC. Figure 5.1 shows example exotherms illustrating the effect of various homogenization methods for T-44 systems. One slurry was mixed at ambient temperature in a speed mixer and stored at sub ambient temperatures until curing. This sample exhibited a mass normalized average heat of reaction of 562.5 J/g and was used to compare and evaluate the effect of other homogenization and sample preparation methods. The results for a T-44 mixture prepared by the *traditional* method, as described

in Chapter II, is shown in Figure 5.1. It is clear reaction is initiated by this method. An average ΔHUC of 488 J/g indicates at least 10% of reaction occurred in the flask prior to any curing or formulation testing. It is also important to note that this false ΔHUC would artificially decreases DOC calculations if it were to be used as representative of the zero point of the reaction. Finally, as is described in the materials preparation section, working with the slurries and filling desired molds require the viscosity to be reduced using a vacuum oven. Slurried samples treated in this manner were also tested to determine if reaction was prematurely initiated. The results indicate that this preparation technique maintains a true zero conversion of the slurry before beginning cure or testing.

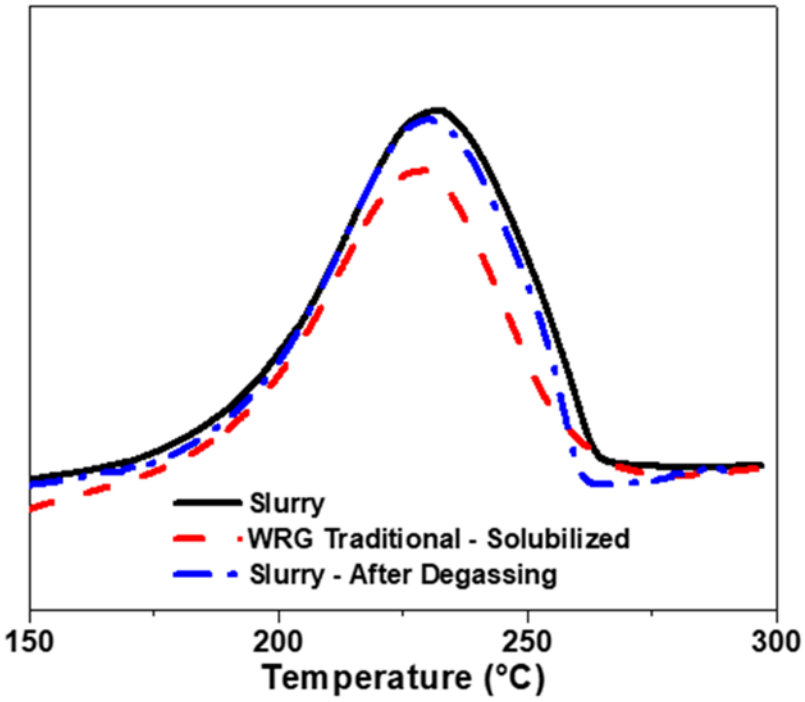

Figure 5.1 Heat of reaction for a freshly mixed slurry compared to the traditional WRG pre-solubilized mixture and in the slurried mixture after reducing viscosity and degassing in a vacuum oven.

5.3 Thermomechanical Properties of T-33 and T-44 Networks

Slurried mixtures of TGDDM/DDS were cured as described in the Chapter II at pre-designated temperature ramp rates. The storage modulus and tan δ plots for the fully cured samples are shown in Figure 5.2. The ultimate T_g for both systems (i.e. the temperature at the maximum point of the tan δ curve) are equivalent regardless of temperature ramp rate (T-33 – 254.53 °C, T-44 – 286.78 °C). A lower peak or shoulder is observed next to the main tan δ peak and appear at the same temperature regardless of the cure protocol used (33DDS – 217.23 °C, 44DDS – 226.69 °C). This temperature sweep method used to probe thermomechanical relaxations of these high T_g glassy thermosets has limitations in fully probing the properties of the cured networks. A commonly reported property of networks is the molecular weight between crosslinks. The calculation of this property requires an accurate value of the rubbery modulus, which is taken as the storage modulus value at a temperature above the T_g. However, for both the TGDDM based networks the onset of degradation occurs at temperatures very near to the ultimate T_g, so we were unable to record an accurate value for the rubbery modulus. Also, both of these high T_g networks vitrify during cure. The lower peaks in both networks most likely represent the T_g of networks as they were cured in the oven and during the thermal ramp within the DMA the samples devitrified and finished cure. This means that we are unable to probe past the T_g of these networks via thermal sweep DMA.

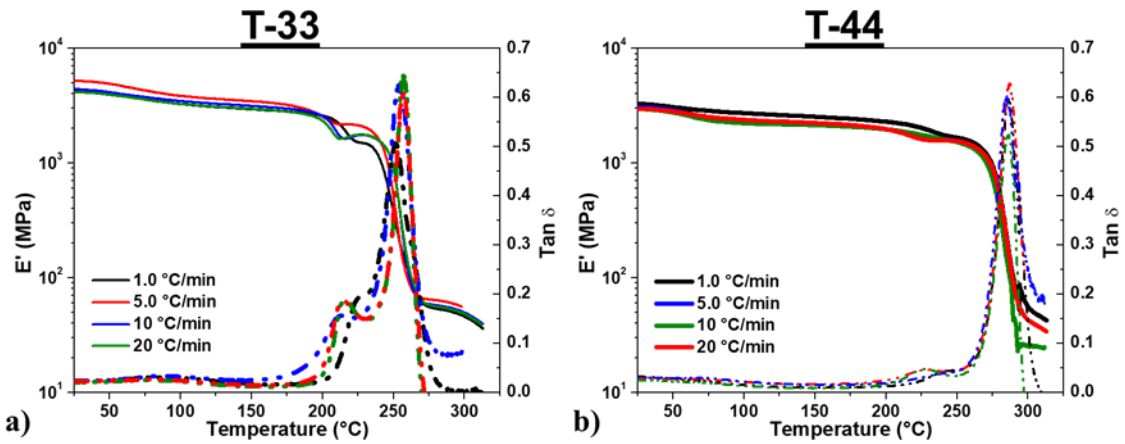

Figure 5.2 Storage modulus and Tan δ data for a) T-33 and b) T-44 networks cured with temperature ramp rates of 1, 5, 10, and 20 °C/min.

Sub-T_g transitions were investigated by acquiring low temperature DMA data (Figures 5.3 and 5.4). As observed in the other DMA work, the temperature ramp rate did not affect the thermomechanical properties of the networks. It is interesting to note that the magnitude of the γ transition in the loss modulus is greater than the α transition for T-44 as compared to the T-33 networks. This is probably due to the ability for the aromatic rings of 44DDS to rotate about an axis and thus to dissipate energy.

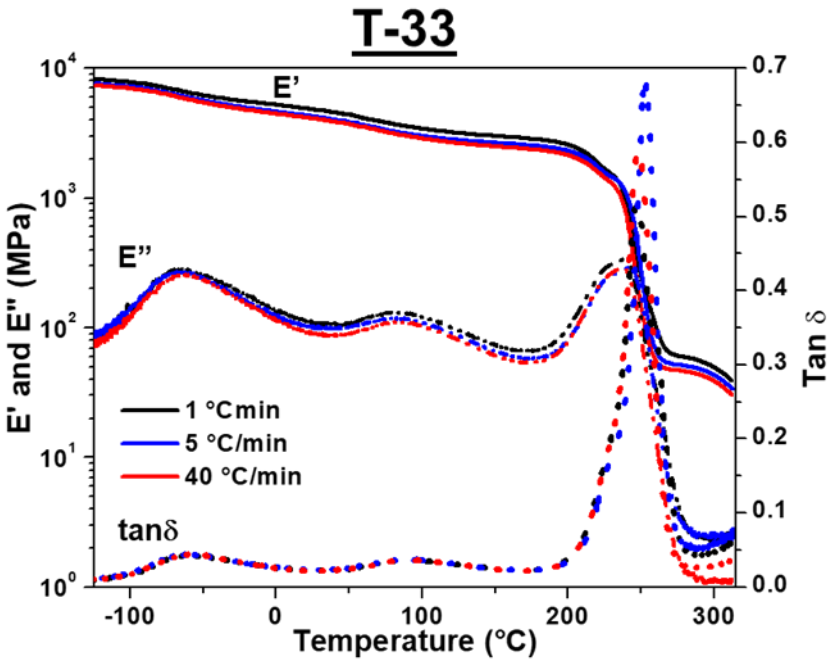

Figure 5.3 Low temperature E', E", and tan δ data for T-33 networks at slow, intermediate, and fast temperature ramp rates.

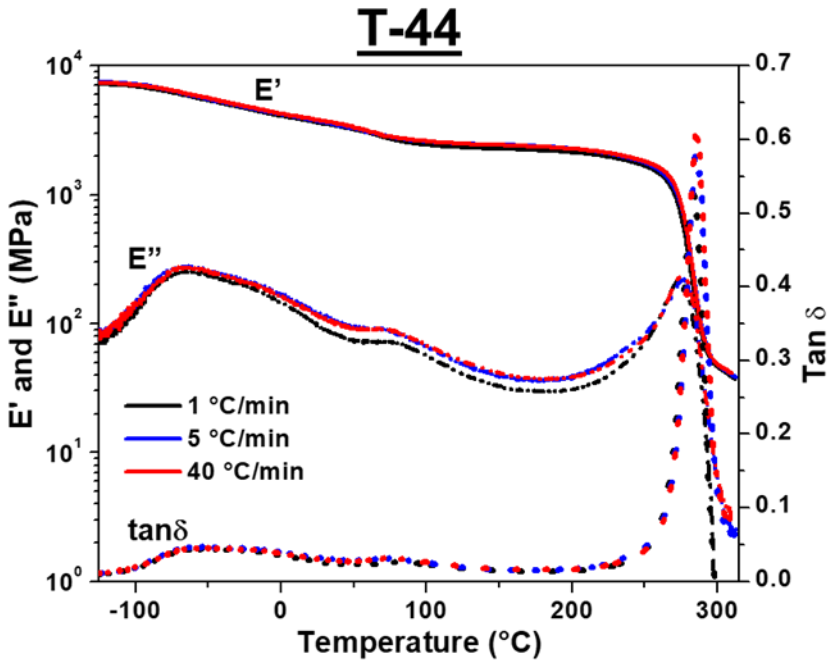

Figure 5.4 Low temperature E', E", and tan δ data for T-44 networks at slow, intermediate, and fast temperature ramp rates.

5.4 Development of Network T_g with Increasing Conversion

Slurried mixtures of TGDDM/DDS were cured in a Modulated DSC cell and held at 180 °C for increasing durations to observe the effect of temperature ramp rate on DOC. Using MDSC allows for the identification of reversible and irreversible thermal transitions. Thus, the instantaneous T_g can be to be directly related to the extent of conversion in the network which can be calculated with the irreversible exotherm of the residual heat of reaction. Here, the instantaneous T_g refers to the T_g of the matrix at the point of quenching. The progression of T_g as a function on isothermal duration can be seen in the set of reversible heat flow curves plotted in Figure 5.5.

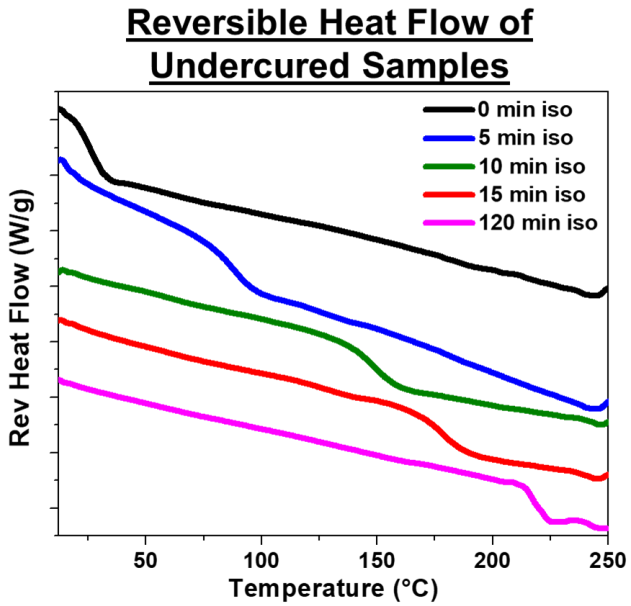

Figure 5.5 Reversible heat flow output from MDSC of a T-33 system showing the increase of T_g of the network when ramped at 10°C/min and held at 180 °C for increasing durations.

The instantaneous T_g of fully and under cured networks were plotted against conversion in order to determine if the cure pathway affected the development of network properties (Figure 5.6). The curve shapes differ for the networks cured with 33DDS and

44DDS, with 33DDS exhibiting a more linear relationship between the extent of conversion and increasing of T_g. Although samples were ramped up to 180°C at different ramp rates, no major difference were observed as the results followed the same trend.

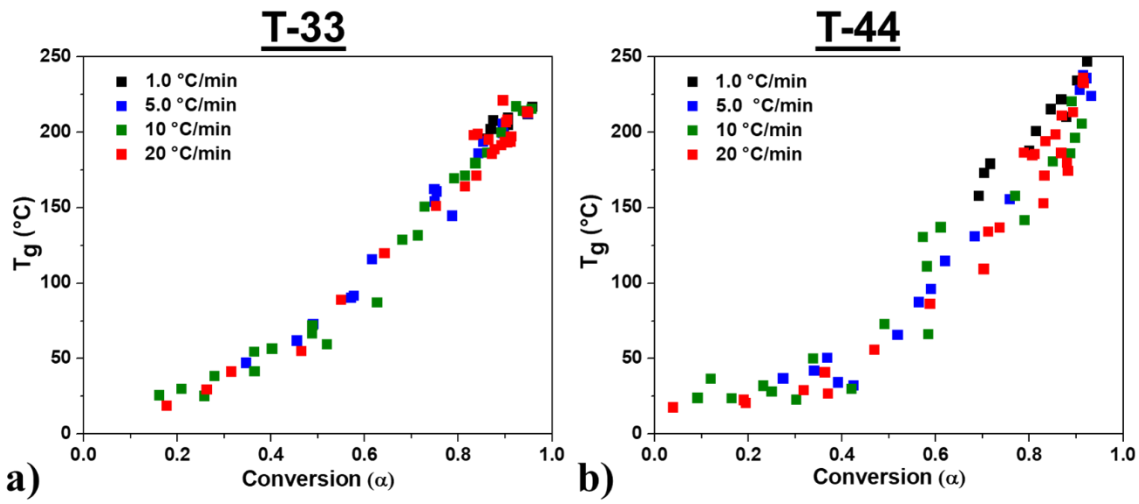

Figure 5.6 T_g vs conversion of a) T-33 and b) T-44 cured with thermal ramp rates of 1, 5, 10, and 20 °C/min and held for different durations at 180°C in order to drive various degrees of cure.

44DDS exhibits a less linear trend, characterized by a slow increase in T_g prior to ~30% conversion. 33DDS is more reactive than 44DDS, so this may explain the results. All cures in the MDSC cell were ramped to 180°C prior to quenching. None of the 1 °C/min thermal ramp protocols produced networks with below 60% DOCs even for protocols with no isothermal hold. This indicates that a majority of cure occurs in these networks curing temperature ramp for the slowest rate studied.

5.5 Thermomechanical Properties of Undercured Networks

DMA samples were cured using different cure protocols to create samples with varied degrees of cure. The DOCs for the cured samples were determined with by residual heat of reaction with DSC. DMA bars of T-33 generally were not sufficiently stiff for DMA analysis at DOC values below 85%; thus, the 33DDS samples exhibited

very little difference in thermomechanical properties of the undercured samples. In contrast, the T-44 samples were able to be cured over a wider span of DOC values. A drop in the low temperature storage modulus was observed for samples having DOC levels of between 60% and 75% DOC. Unfortunately, a sample with a DOC value between those limits could not be produced; obtaining such a sample is a possible future goal for this project.

The large span of DOCs obtained for the T-44 networks allowed for a deeper investigation into the thermomechanical properties of these networks as a function of cure. Figure 5.7 shows the tan δ data for T-44 networks cured to different DOC levels. Note the higher temperature peaks are basically identical in shape and position with the fully cured T-44 networks. This indicates post curing is occurring during data acquisition. This is further verified by MDSC analysis of the cured DMA bars which show that the T_g in the reversible heat flow is far below the ultimate tan δ peak (Figure 5.8). In fact, the instantaneous T_g determined using MDSC matches the initial tan δ peak of the undercured T-44 network.

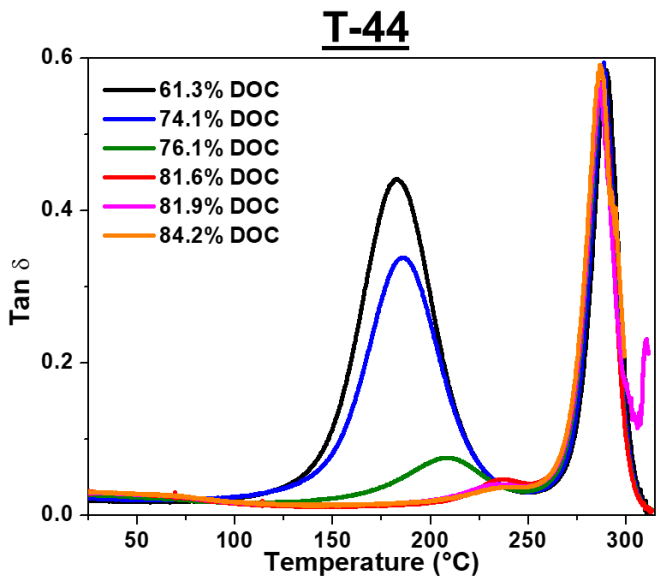

Figure 5.7 Tan δ plots of T-44 samples undercured to various degrees of cure.

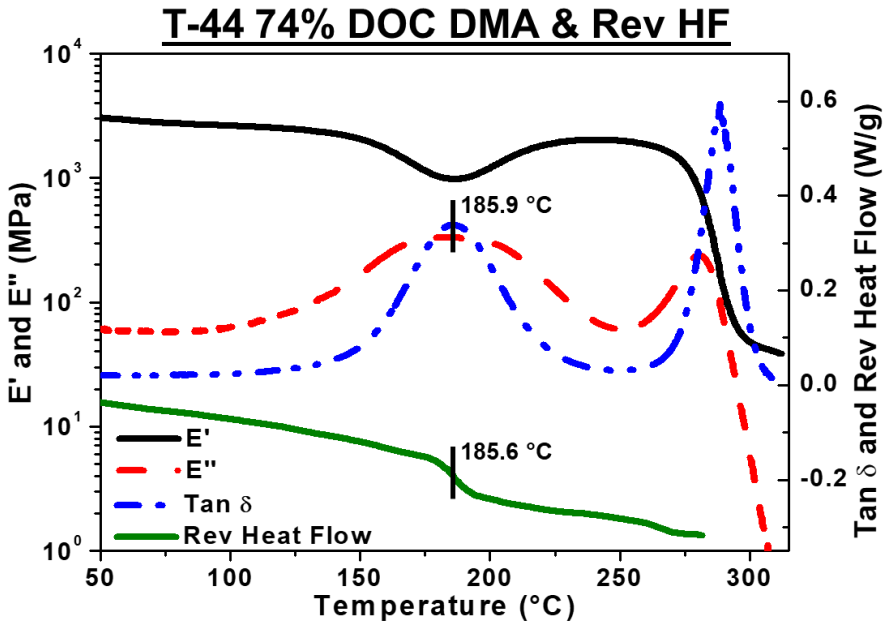

Figure 5.8 DMA data for undercured T-44 (74% DOC) compared to the reversible heat flow of the same sample obtained with MDSC with the network's instantaneous T_g identified.

5.6 Considerations of Rapid Curing Thermosets in Convection Ovens

The main goal of this work is to identify and quantify potential differences in epoxy/diamine networks when cured using increasing temperature ramp rates. This has

done using a variety of thermal, thermomechanical, and spectroscopic techniques. It is normally assumed that curing of small volumes of slurry in DSC and RT-NIR instruments mimic the cure larger samples performed in an oven and then removed for analysis by DMA or other mechanical methods. Additionally, in previous work it was assumed that the actual temperature ramp rate of the systems cured by these different methods match the targeted protocols. To test this assumption, the actual matrix temperature during cure in the oven was monitored. Temperature versus time readings were collected using a Four-Channel Handheld Data Logger Thermometer (OMEGA HH147U) capable of simultaneously recording data from four discrete thermocouples simultaneously. Thermocouples were placed outside as well as within the matrices being cured.

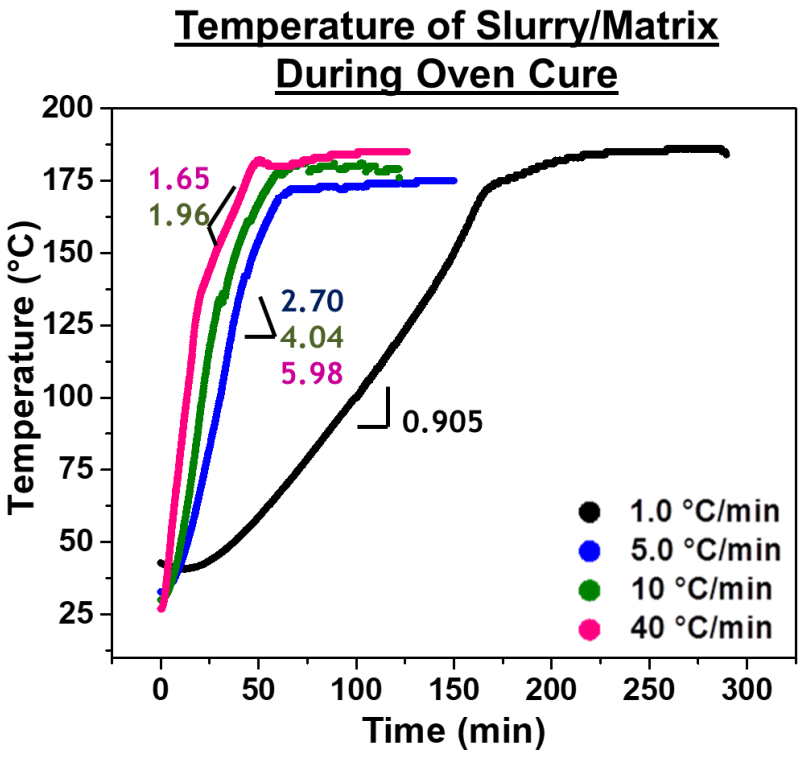

Figure 5.9 Temperature readings for the matrix while curing within the programmable oven.

Figure 5.9 shows data collected from thermocouples placed in slurry during cure. The temperature of the curing network is very different from the programmed rate of the convection oven. There is a noticeable slope change for the faster ramp rates, so the initial and secondary slopes of these cures are both identified in Figure 5.9. Previously it was determined that the oven needed to be set to a higher target temperature in order to obtain an actual oven temperature of 180 °C. These observations suggest that the actual matrix heating rates did not match the programmed protocol values, thereby making data acquired using samples cured in the ovens such as DMA questionable. This may explain the similarity of the observed thermomechanical properties of the networks cured with increasingly fast protocols. The fastest targeted rate (40 °C) initially has a maximum thermal ramp rate of ~6 °C/min for first 20 minutes, after which point the rate decreases. This implies that these sample's properties are for a network cured at an average thermal ramp rate to the isotherm of ~3 °C/min (Table 5.1).

Table 5.1 True Temperature Ramp Rates of Oven Cured Matrix.

Programmed Rate (°C/min)	Initial Slope (°C/min)	Average rate to reach isotherm (°C/min)
40	5.98	3.19
10	4.04	2.71
5	2.70	2.23
1	0.91	0.85

5.7 F-33 vs T-33

F-33 and T-33 networks were compared using maximum temperature ramp rates of 5 °C/min due to the limitations of the oven cure process. The F-33 networks offer potential differences compared to T-33 systems. The lower average functionality of the

monomers should reduce the crosslink density; thus, gelation is expected to occur at a higher DOC and thereby permit more of the reaction to occur due to the functional groups having higher mobility. Also, the ultimate T_g of F-33 is lower than the 180 °C cure temperature, which should allow for 100% cure. The tan δ of the F-33 and T-33 networks are displayed in Figure 5.10. The T_gs of the F-33 networks were unaffected (~157 °C) as were the instantaneous T_gs of the T-33 networks (~231 °C). As previously observed, the ultimate T_g of the T-33 networks cured by each protocol were equivalent. The unimodal tan δ peak for the F-33 systems indicates that the ultimate T_g of the network was reached when cured with each thermal protocol. There appears to be slight broadening of the tan δ peak for the 5.0 °C/min thermal ramp rate cure, which may indicate a higher degree of heterogeneity in the network architecture for that system.

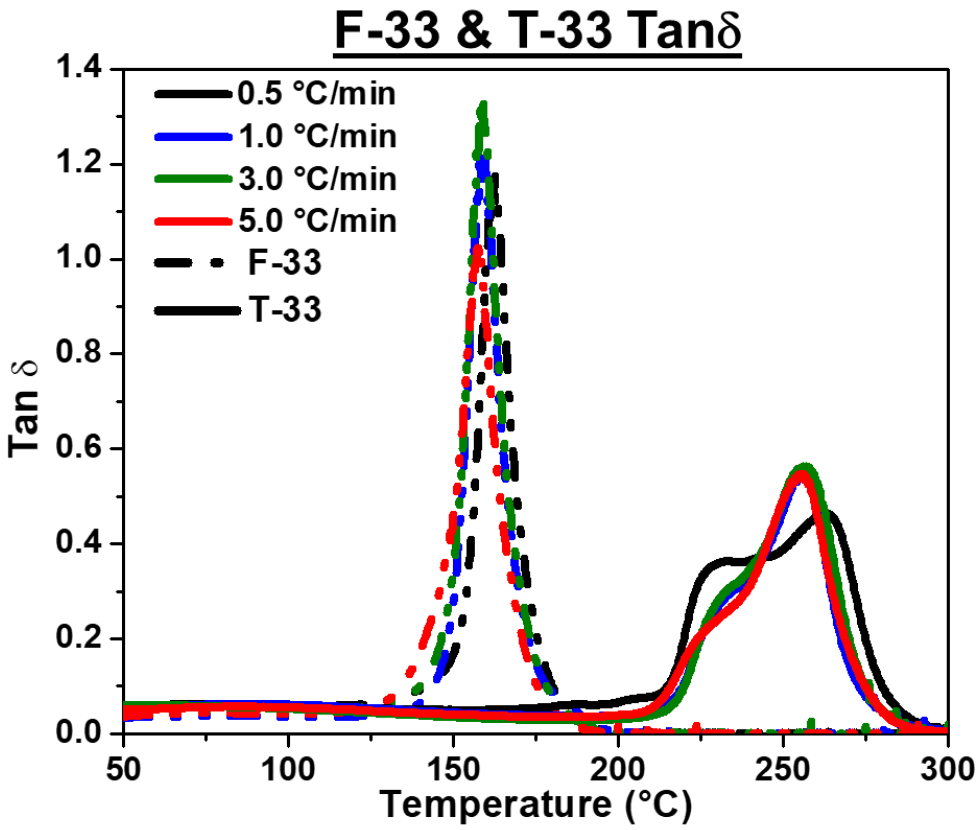

Figure 5.10 Tan δ of F-33 and T-33 networks cured using temperature ramp rates of 0.5, 1, 3, and 5 °C/min.

The F-33 and T-33 samples were both placed in refluxing DI water for 24 hours as described in Chapter II to determine if cure rate affected free hole space. The results shown in Table 5.2 indicate no effect caused by different cure protocols.

Table 5.2 Percent Mass Increase After Swelling with DI Water.

Network	0.5 °C/min	1.0 °C/min	3.0 °C/min	5.0 °C/min
	Mass Increase (%)			
F-33	2.84 ± 0.0531	2.67 ± 0.0573	2.53 ± 0.106	2.61 ± 0.168
T-33	3.71 ± 0.0402	4.21 ± 0.150	4.02 ± 0.110	4.08 ± 0.212

Figure 5.11 shows the stress/strain curves for the F-33 and T-33 networks. The data shows cure protocols do not significantly affect the mechanical properties. It appears that after the full 2-hour 180 °C isotherm the network connectivity in both networks

indistinguishable when cured with different thermal ramp rates. The Young's modulus and yield stress are listed in Table 5.3.

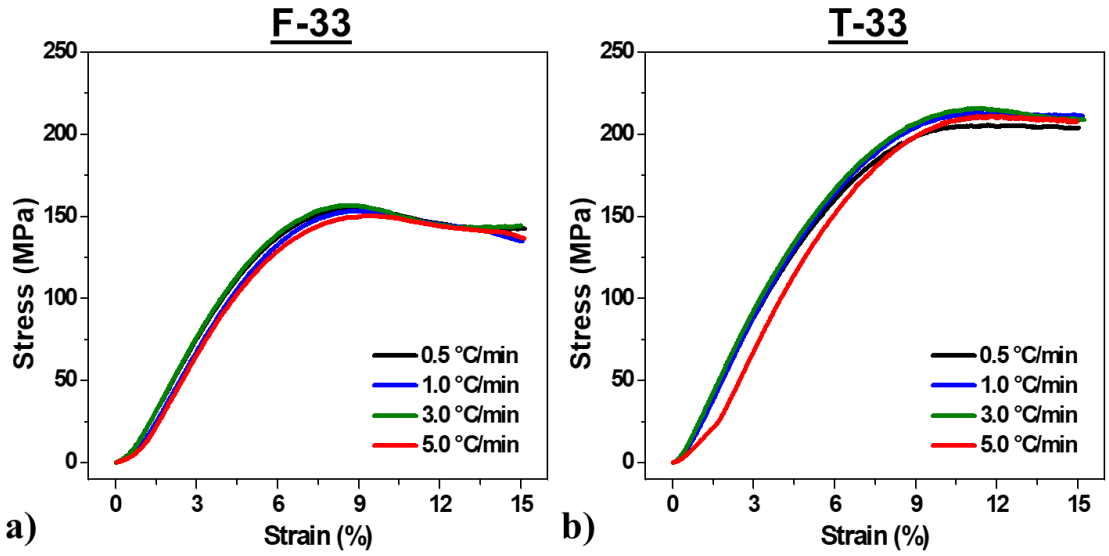

Figure 5.11 Stress vs. strain mechanical data collected in compression mode for a) F-33 and b) T-33 networks cured with thermal ramp rates of 0.5, 1, 3, and 5 °C/min.

Table 5.3 Young's Modulus and Yield Stress from Compressive Mechanical Tests of F-33 and T-33 Networks.

Network	0.5 °C/min	1.0 °C/min	3.0 °C/min	5.0 °C/min
	Young's Modulus (GPa)			
F-33	2.99	2.90	3.04	2.93
T-33	3.39	3.42	3.39	3.39
	Yield Stress (MPa)			
F-33	115.16	153.21	156.6	150.55
T-33	205.35	213.04	211.13	205.35

5.8 Comparison of Rheologic Data to RT-NIR Results

Oscillatory shear rheological profiles up to gelation were acquired for the F-33 and T-33 systems cured at various ramp rates to determine if the development of the viscoelastic properties is related to the different network growth pathways observed in

RT-NIR analysis. For this study F-33 and T-33 samples were cured using temperature ramp rates of 1, 3, or 5 °C/min in the rheometer and the RT-FTIR spectrometer.

The gelation time marks the onset of the diffusion restricted reaction kinetics, as material behavior transitions from being dominated by a liquid-like, viscous response to a solid-like, elastic response. As shown in Figures 5.12 and 5.13, increasing the temperature ramp rate from 1 °C/min to 5 °C/min affects the time to gelation for both the T-33 and F-33 system. Tables 5.4 through 5.6 summarize the rheological results.

Table 5.4 Points of Interest at the Gel Point of F-33 and T-33 Networks Cured Using a Temperature Ramp Rate of 1 °C/min.

Network	1 °C/min		
	Complete A' Consumption (min)	Gel Time (min)	Viscosity at Gel Point (Pa.s)
F-33	132	139.1	7.9
T-33	138	139.1	161.0

Table 5.5 Points of Interest at the Gel Point of F-33 and T-33 Networks Cured Using a Temperature Ramp Rate of 3 °C/min.

Network	3 °C/min		
	Complete A' Consumption (min)	Gel Time (min)	Viscosity at Gel Point (Pa.s)
F-33	54	59.6	9.3
T-33	56	55.2	132.6

Table 5.6 Points of Interest at the Gel Point of F-33 and T-33 Networks Cured Using a Temperature Ramp Rate of 5 °C/min.

Network	5 °C/min		
	Complete A' Consumption (min)	Gel Time (min)	Viscosity at Gel Point (Pa.s)
F-33	35	35.2	2.6
T-33	45	36.9	67.9

For both networks, the 1 °C/min ramp rate was the only cure protocol whereby gelation occurred before the 180°C isotherm was reached. This creates longer dwell times in more diffusive environments for the reactants at the lower temperature ramps, thereby yielding a higher conversion of primary amine at or before the gel point.

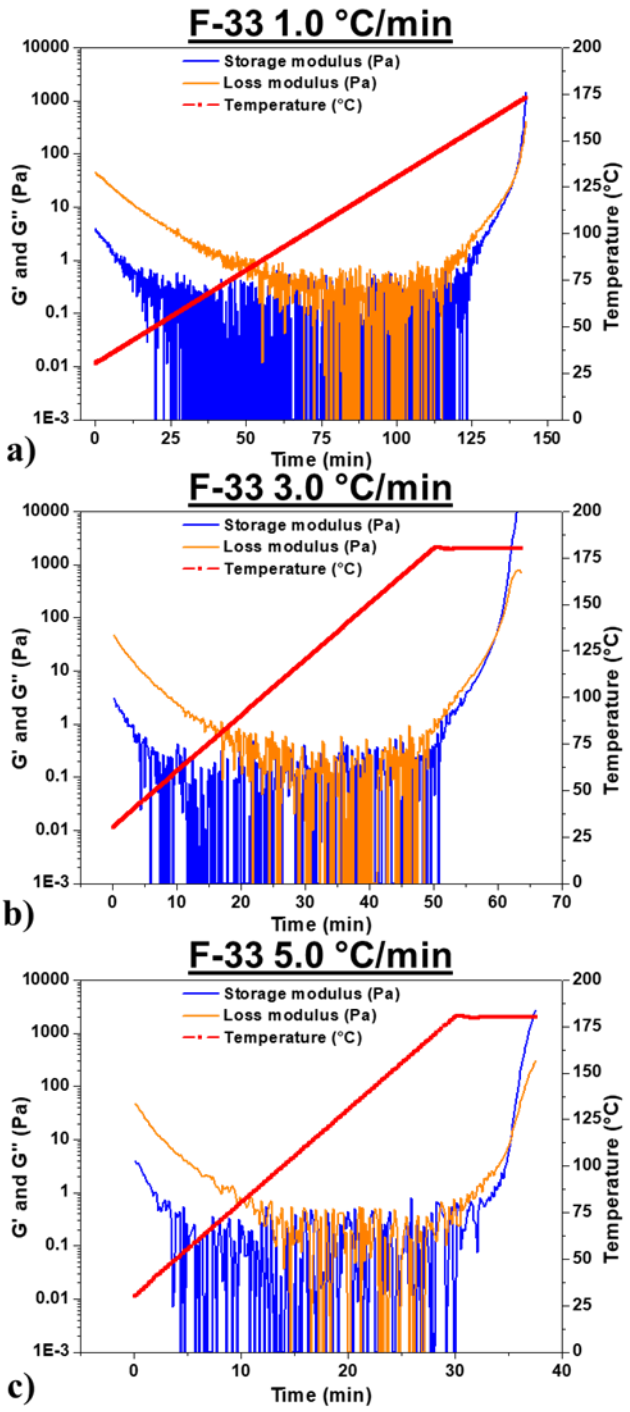

Figure 5.12 Crossover of G’ and G” for the F-33 network cure with temperature ramp rates of 1, 3, and 5 °C/min.

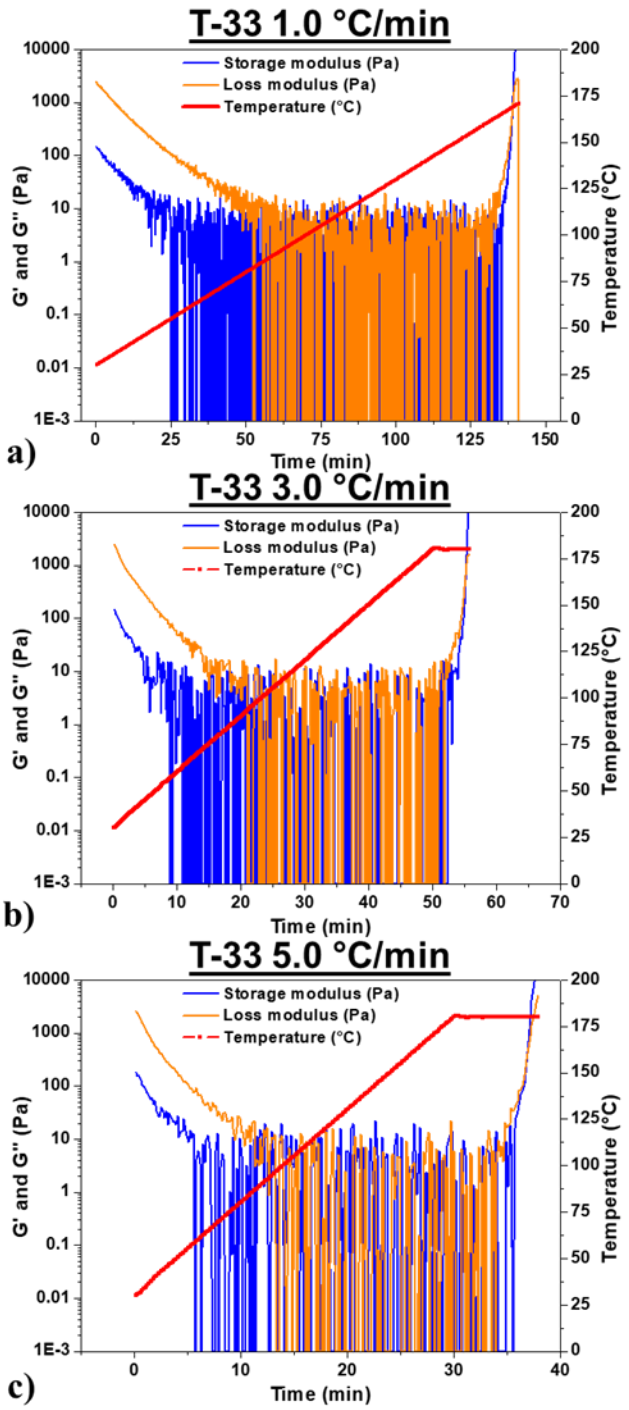

Figure 5.13 Crossover of G’ and G” for the T-33 network cure with temperature ramp rates of 1, 3, and 5 °C/min.

The above tables show a trend in the F-33 systems involving time to gelation and the time until complete primary amine consumption via RT-NIR analysis. All primary amines have reacted before gelation occurs for each F-33 cure path; this indicates linear chain growth is the dominant mechanism prior to gelation. However, upon consumption of primary amines gelation rapidly occurs due to crosslinked formed by the reacting secondary amines. Furthermore, the viscosity at the point of gelation is extremely low (Figure 5.14) for the F-33 systems, which correlates with the low amount of secondary amines that have been reacted into the system at that point limiting the degree of crosslinking early in cure (Figure 5.16). The data also suggests that the low viscosity of the system allows for primary amines to remain more reactive than secondary amines thus resulting in the near theoretical maximum concentration of the secondary amines observed in RT-NIR analysis.

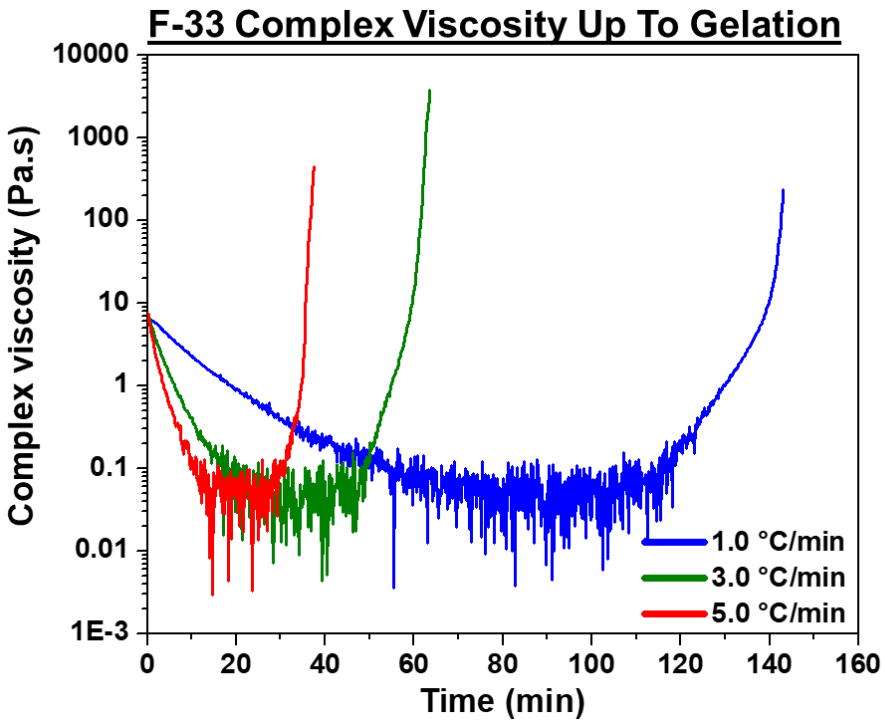

Figure 5.14 Complex viscosity of F-33 systems up to the gel point for temperature ramp rates of 1, 3, and 5 °C/min.

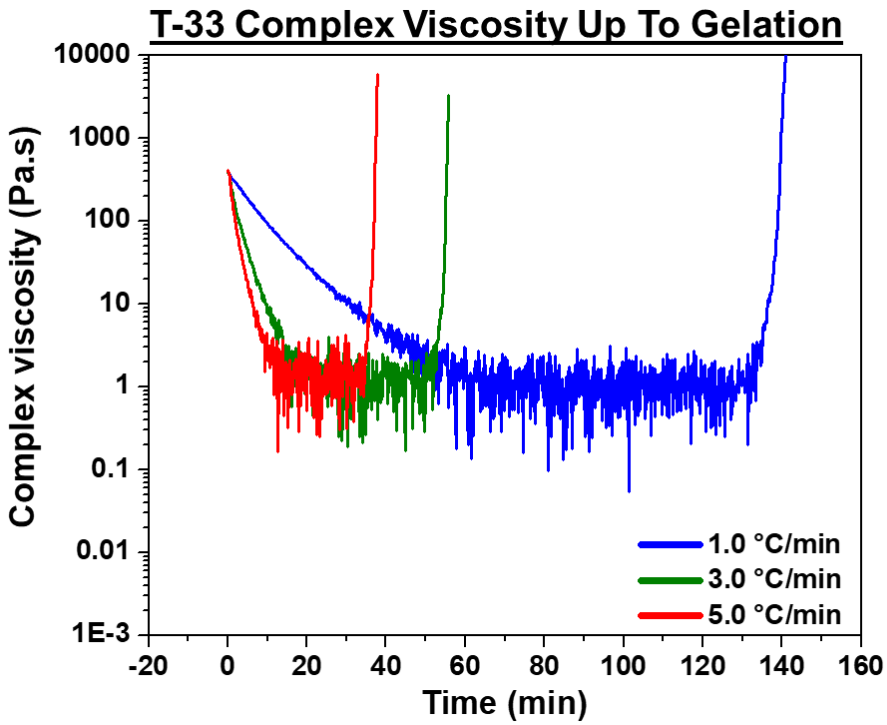

Figure 5.15 Complex viscosity of T-33 systems up to the gel point for temperature ramp rates of 1, 3, and 5 °C/min.

In the T-33 systems, using a 1 °C/min ramp rate, all the primary amines were reacted immediately preceding gelation. However, for the higher ramp rates gelation preceded the complete consumption of primary amines. This effect is quite clearly observed at the highest ramp rate, where gelation occurred approximately 8 minutes before the total primary amine consumption. The viscosity at gelation for the T-33 system exhibited a trend similar to that observed for the F-33 system, with the concentration of secondary amines at gelation correlating directly with viscosity.

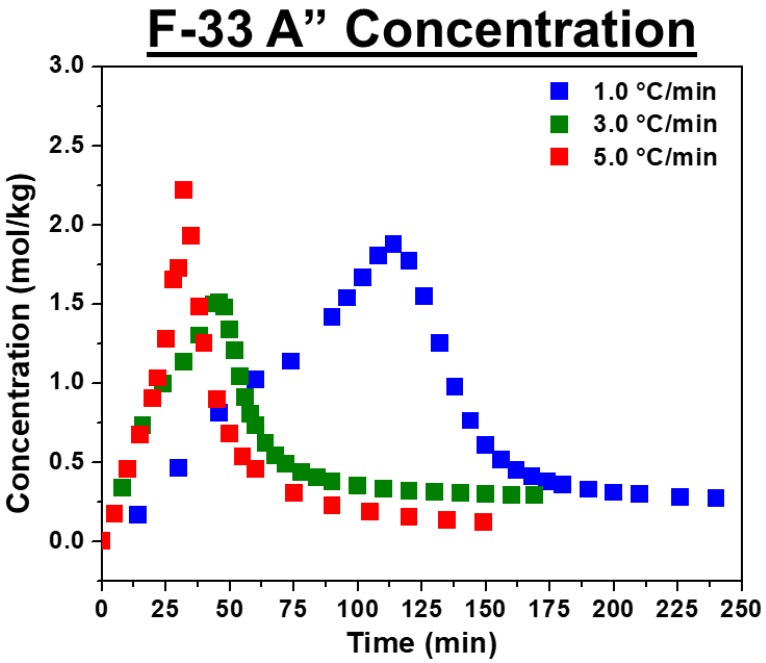

Figure 5.16 Concentration of secondary amine versus time of F-33 systems cured with thermal ramp rates of 1, 3 and 5 °C/min.

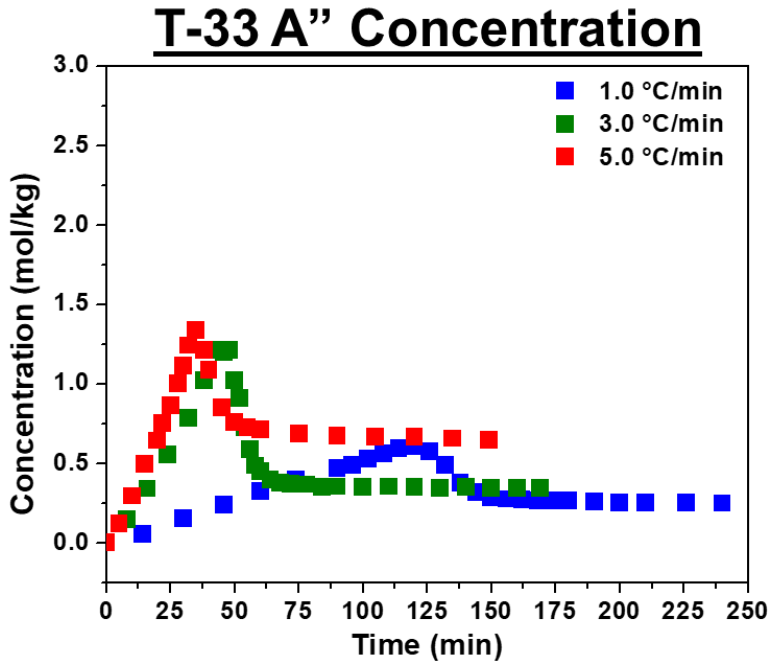

Figure 5.17 Concentration of secondary amine versus time of F-33 systems cured with thermal ramp rates of 1, 3 and 5 °C/min.

It is interesting to compare RT-NIR data concerning the pathway of network formation to the development of network properties as determined by rheometry. First, it should be noted, the order of magnitude difference in viscosity between the F-33 and T-33 systems in their minimum viscosity states prior to gelation (Figures 5.14 and 5.15). Prior to the storage and loss modulus crossover event, the F-33 system is in a more diffuse environment for the epoxide/amine reactions to occur. Also, a higher maximum concentration of secondary amines is observed; this suggests linear growth prior to secondary amine reaction (Figure 5.16). In the higher viscosity T-33 system, a lower maximum secondary amine concentration is observed, indicating the effect viscosity has on the competitive reaction between secondary amine and primary amines. The loss of molecular freedom promotes local secondary amine consumption due to the lack of network mobility. This behavior is supported by both the RT-NIR and rheological data.

5.9 Conclusions and Future Work

The final macroscopic mechanical and thermomechanical properties of all the networks studied were not affected by the thermal ramp rate applied during cure. The RT-FTIR results prove that the pathway in which the networks form is affected by the cure protocol. However, the consequence of those different pathways is not apparent based on the macroscopic properties tested on the cured networks. One hypothesis based on the results suggest the length of time spent at 180 °C drives the networks, regardless of cure protocols used, to a level of connectivity and cohesiveness such that the resulting macroscopic properties are indistinguishable from each other.

It is possible that there is an effect on the matrix that has yet to be probed. The probable best way to probe tangible network material property effects of cure protocol is

to study systems in various states of undercure. It must be noted that the tests cannot progress the reaction, as a thermal sweep observed for DMA analysis does or the potential changes in matrix properties will be obscured. Additionally, long term effects on network properties were not studied in this work. Investigations into fatigue properties or solvent uptake over an extended time may elucidate effects imparted on epoxy/diamine networks cured with increasing thermal ramp rates.

REFERENCES

(1) Rozenberg, B. A. Kinetics, Thermodynamics and Mechanism of Reactions of Epoxy Oligomers with Amines. In *Epoxy resins and composites II*; Springer, 1986; pp 113–165.

(2) Odian, G. *Principles of Polymerization*; John Wiley & Sons, 2004.

(3) Smith, M. B.; March, J. *March's Advanced Organic Chemistry: Reactions, Mechanisms, and Structure*; John Wiley & Sons, 2007.

(4) Kuo, S.-W.; Chang, F.-C. POSS Related Polymer Nanocomposites. *Prog. Polym. Sci.* **2011**, *36* (12), 1649–1696.

(5) Guadagno, L.; Vertuccio, L.; Sorrentino, A.; Raimondo, M.; Naddeo, C.; Vittoria, V.; Iannuzzo, G.; Calvi, E.; Russo, S. Mechanical and Barrier Properties of Epoxy Resin Filled with Multi-Walled Carbon Nanotubes. *Carbon N. Y.* **2009**, *47* (10), 2419–2430.

(6) Meyer, F.; Sanz, G.; Eceiza, A.; Mondragon, I.; Mijović, J. The Effect of Stoichiometry and Thermal History during Cure on Structure and Properties of Epoxy Networks. *Polymer (Guildf).* **1995**, *36* (7), 1407–1414.

(7) Sohn, D. W.; Ko, K. J. A Study on the Characterization of Etherification in Diamine Cured Epoxy System. *Korea Polym. J.* **1999**, *7* (3), 181–188.

(8) Sherman, C. L.; Zeigler, R. C.; Verghese, N. E.; Marks, M. J. Structure–property Relationships of Controlled Epoxy Networks with Quantified Levels of Excess Epoxy Etherification. *Polymer (Guildf).* **2008**, *49* (5), 1164–1172.

(9) Ophir, Z. H.; Emerson, J. A.; Wilkes, G. L. Sub-T g Annealing Studies of Rubber-modified and Unmodified Epoxy Systems. *J. Appl. Phys.* **1978**, *49* (10), 5032–5038.

(10) Apicella, A.; Masi, P.; Nicolais, L. Rheological Behaviour of a Commercial TGDDM-DDS Based Epoxy Matrix during the Isothermal Cure. *Rheol. acta* **1984**, *23* (3), 291–296.

(11) Hou, T. H.; Huang, J. Y. Z.; Hinkley, J. A. Chemorheology of an Epoxy Resin System under Isothermal Curing. *J. Appl. Polym. Sci.* **1990**, *41* (3-4), 819–834.

(12) Vyazovkin, S.; Sbirrazzuoli, N. Mechanism and Kinetics of Epoxy− Amine Cure Studied by Differential Scanning Calorimetry. *Macromolecules* **1996**, *29* (6), 1867–1873.

(13) Roşu, D.; Caşcaval, C. N.; Mustată, F.; Ciobanu, C. Cure Kinetics of Epoxy Resins Studied by Non-Isothermal DSC Data. *Thermochim. Acta* **2002**, *383* (1–2), 119–

127.

(14) Jacobson, H.; Stockmayer, W. H. Intramolecular Reaction in Polycondensations. I. The Theory of Linear Systems. *J. Chem. Phys.* **1950**, *18* (12), 1600–1606.

(15) Lubin, G. *Handbook of Composites*; Springer Science & Business Media, 2013.

(16) Deng, Y.; Martin, G. C. Modeling Diffusion during Thermoset Cure: An Approach Based on Dielectric Analysis. *Macromolecules* **1994**, *27* (18), 5141–5146.

(17) De Gennes, P. G. Kinetics of Diffusion-controlled Processes in Dense Polymer Systems. I. Nonentangled Regimes. *J. Chem. Phys.* **1982**, *76* (6), 3316–3321.

(18) Deng, Y.; Martin, G. C. Diffusion and Diffusion-Controlled Kinetics during Epoxy-Amine Cure. *Macromolecules* **1994**, *27* (18), 5147–5153.

(19) Carbas, R. J. C.; Da Silva, L. F. M.; Marques, E. A. S.; Lopes, A. M. Effect of Post-Cure on the Glass Transition Temperature and Mechanical Properties of Epoxy Adhesives. *J. Adhes. Sci. Technol.* **2013**, *27* (23), 2542–2557.

(20) Mostovoy, S.; Ripling, E. J. Fracture Toughness of an Epoxy System. *J. Appl. Polym. Sci.* **1966**, *10* (9), 1351–1371.

(21) Hiemenz, P. C.; Lodge, T. P. *Polymer Chemistry*; CRC press, 2007.

(22) Lesser, A. J.; Calzia, K. J. Molecular Parameters Governing the Yield Response of Epoxy-based Glassy Networks. *J. Polym. Sci. Part B Polym. Phys.* **2004**, *42* (11), 2050–2056.

(23) Bershtein, V. A.; Peschanskaya, N. N.; Halary, J. L.; Monnerie, L. The Sub-Tg Relaxations in Pure and Antiplasticized Model Epoxy Networks as Studied by High Resolution Creep Rate Spectroscopy. *Polymer (Guildf).* **1999**, *40* (24), 6687–6698.

(24) Heinz, S. R.; Wiggins, J. S. Uniaxial Compression Analysis of Glassy Polymer Networks Using Digital Image Correlation. *Polym. Test.* **2010**, *29* (8), 925–932.

(25) Oleinik, E. F. Epoxy-Aromatic Amine Networks in the Glassy State Structure and Properties. In *Epoxy resins and composites IV*; Springer, 1986; pp 49–99.

(26) Jackson, M.; Kaushik, M.; Nazarenko, S.; Ward, S.; Maskell, R.; Wiggins, J. Effect of Free Volume Hole-Size on Fluid Ingress of Glassy Epoxy Networks. *Polymer (Guildf).* **2011**, *52* (20), 4528–4535.

(27) Frank, K. L. Relationships between Cure Kinetics, Network Architecture, and Fluid Sensitivity in Glassy Epoxies. **2013**.

(28) Frank, K.; Childers, C.; Dutta, D.; Gidley, D.; Jackson, M.; Ward, S.; Maskell, R.; Wiggins, J. Fluid Uptake Behavior of Multifunctional Epoxy Blends. *Polymer (Guildf).* **2013**, *54* (1), 403–410.

(29) Childers, C. H.; Hassan, M. K.; Mauritz, K. A.; Wiggins, J. S. Molecular Scale Cure Rate Dependence of Thermoset Matrix Polymers. *Arab. J. Chem.* **2016**, *9* (2), 206–218.

(30) Carter, J. T.; Emmerson, G. T.; Faro, C. Lo; McGrail, P. T.; Moore, D. R. The Development of a Low Temperature Cure Modified Epoxy Resin System for Aerospace Composites. *Compos. Part A Appl. Sci. Manuf.* **2003**, *34* (1), 83–91.

(31) Frank, K. L.; Exley, S. E.; Thornell, T. L.; Morgan, S. E.; Wiggins, J. S. Investigation of Pre-Reaction and Cure Temperature on Multiscale Dispersion in POSS–epoxy Nanocomposites. *Polymer (Guildf).* **2012**, *53* (21), 4643–4651.

(32) Kazilas, M. C.; Partridge, I. K. Exploring Equivalence of Information from Dielectric and Calorimetric Measurements of Thermoset Cure—a Model for the Relationship between Curing Temperature, Degree of Cure and Electrical Impedance. *Polymer (Guildf).* **2005**, *46* (16), 5868–5878.

(33) Jackson, M. B. Effects of Molecular Architecture on Fluid Ingress Behavior of Glassy Polymer Networks. **2011**.

(34) Knowles, K. R. Effect of Chain Rigidity on Network Architecture and Deformation Behavior of Glassy Polymer Networks. **2017**.

(35) Stutz, H.; Illers, K.; Mertes, J. A Generalized Theory for the Glass Transition Temperature of Crosslinked and Uncrosslinked Polymers. *J. Polym. Sci. Part B Polym. Phys.* **1990**, *28* (9), 1483–1498.

(36) Lesser, A. J.; Crawford, E. The Role of Network Architecture on the Glass Transition Temperature of Epoxy Resins. *J. Appl. Polym. Sci.* **1997**, *66* (2), 387–395.

(37) Cizmecioglu, M.; Gupta, A.; Fedors, R. F. Influence of Cure Conditions on Glass Transition Temperature and Density of an Epoxy Resin. *J. Appl. Polym. Sci.* **1986**, *32* (8), 6177–6190.

(38) Varley, R. J.; Liu, W.; Simon, G. P. Investigation of the Reaction Mechanism of Different Epoxy Resins Using a Phosphorus-based Hardener. *J. Appl. Polym. Sci.* **2006**, *99* (6), 3288–3299.

(39) Vanlandingham, M. R.; Eduljee, R. F.; Gillespie Jr, J. W. Relationships between Stoichiometry, Microstructure, and Properties for Amine-cured Epoxies. *J. Appl. Polym. Sci.* **1999**, *71* (5), 699–712.

(40) Garg, A. C.; Mai, Y.-W. Failure Mechanisms in Toughened Epoxy Resins—A Review. *Compos. Sci. Technol.* **1988**, *31* (3), 179–223.

(41) Botelho, E. C.; Silva, R. A.; Pardini, L. C.; Rezende, M. C. A Review on the Development and Properties of Continuous Fiber/Epoxy/Aluminum Hybrid Composites for Aircraft Structures. *Mater. Res.* **2006**, *9* (3), 247–256.

(42) Azeez, A. A.; Rhee, K. Y.; Park, S. J.; Hui, D. Epoxy Clay Nanocomposites–processing, Properties and Applications: A Review. *Compos. Part B Eng.* **2013**, *45* (1), 308–320.

(43) Tu, J.; Tucker, S. J.; Christensen, S.; Sayed, A. R.; Jarrett, W. L.; Wiggins, J. S. Phenylene Ring Motions in Isomeric Glassy Epoxy Networks and Their Contributions to Thermal and Mechanical Properties. *Macromolecules* **2015**, *48* (6), 1748–1758.

(44) Dušek, K.; Pleštil, J.; Lednický, F.; Luňák, S. Are Cured Epoxy Resins Inhomogeneous? *Polymer (Guildf).* **1978**, *19* (4), 393–397.

(45) Jin, F.-L.; Li, X.; Park, S.-J. Synthesis and Application of Epoxy Resins: A Review. *J. Ind. Eng. Chem.* **2015**, *29*, 1–11.

(46) Haba, D.; Kaufmann, J.; Brunner, A. J.; Resch, K.; Teichert, C. Observation of Elastic Modulus Inhomogeneities in Thermosetting Epoxies Using AFM–Discerning Facts and Artifacts. *Polymer (Guildf).* **2014**, *55* (16), 4032–4040.

(47) Bahrami, A.; Morelle, X.; Pardoen, T.; Bailly, C.; Nysten, B. Curing Dependent Spatial Heterogeneity of Mechanical Response in Epoxy Resins Revealed by Atomic Force Microscopy. *Polymer (Guildf).* **2015**, *68*, 1–10.

(48) Foster, S. F.; Hoff, E. A.; Curtzwiler, G. W.; Williams, E. B.; Davis, K. B.; Patton, D. L.; Rawlins, J. W. Chemorheology Investigation of a Glassy Epoxy Thermoset on Tensile Plastic Flow and Fracture Morphology. *J. Polym. Sci. Part B Polym. Phys.* **2015**, *53* (19), 1333–1344.

(49) Trappe, V.; Günzel, S.; Hickmann, S. Non-Destructive Evaluation of Micro Cracking in Short Fibre Reinforced Thermoplastics with X-Ray-Refraction. In *17th Int. Conf. on Composite Materials*; 2009.

(50) Trappe, V.; Günzel, S.; Jaunich, M. Correlation between Crack Propagation Rate and Cure Process of Epoxy Resins. *Polym. Test.* **2012**, *31* (5), 654–659.

(51) Barton, J. M. The Application of Differential Scanning Calorimetry (DSC) to the Study of Epoxy Resin Curing Reactions. In *Epoxy resins and composites I*; Springer, 1985; pp 111–154.

(52) Gupta, V. B.; Drzal, L. T.; Lee, C.; Rich, M. J. The Temperature-dependence of

Some Mechanical Properties of a Cured Epoxy Resin System. *Polym. Eng. Sci.* **1985**, *25* (13), 812–823.

(53) Hardis, R.; Jessop, J. L. P.; Peters, F. E.; Kessler, M. R. Cure Kinetics Characterization and Monitoring of an Epoxy Resin Using DSC, Raman Spectroscopy, and DEA. *Compos. Part A Appl. Sci. Manuf.* **2013**, *49*, 100–108.

(54) Abliz, D.; Duan, Y.; Steuernagel, L.; Xie, L.; Li, D.; Ziegmann, G. Curing Methods for Advanced Polymer Composites-a Review. *Polym. Polym. Compos.* **2013**, *21* (6), 341–348.

(55) Kratz, J.; Hsiao, K.; Fernlund, G.; Hubert, P. Thermal Models for MTM45-1 and Cycom 5320 out-of-Autoclave Prepreg Resins. *J. Compos. Mater.* **2013**, *47* (3), 341–352.

(56) Centea, T.; Grunenfelder, L. K.; Nutt, S. R. A Review of Out-of-Autoclave Prepregs–Material Properties, Process Phenomena, and Manufacturing Considerations. *Compos. Part A Appl. Sci. Manuf.* **2015**, *70*, 132–154.

(57) Miller, C. E. Near-Infrared Spectroscopy of Synthetic Polymers. *Appl. Spectrosc. Rev.* **1991**, *26* (4), 277–339.

(58) Fu, J. H.; Schlup, J. R. Mid-and Near-infrared Spectroscopic Investigations of Reactions between Phenyl Glycidyl Ether (PGE) and Aromatic Amines. *J. Appl. Polym. Sci.* **1993**, *49* (2), 219–227.

(59) Mertzel, E.; Koenig, J. L. Application of FT-IR and NMR to Epoxy Resins. In *Epoxy Resins and Composites II*; Springer, 1986; pp 73–112.

(60) Dannenberg, H. Determination of Functional Groups in Epoxy Resins by Near-infrared Spectroscopy. *Polym. Eng. Sci.* **1963**, *3* (1), 78–88.

(61) Pramanik, M.; Mendon, S. K.; Rawlins, J. W. Disecondary Amine Synthesis and Its Reaction Kinetics with Epoxy Prepolymers. *J. Appl. Polym. Sci.* **2012**, *126* (6), 1929–1940.

(62) Pramanik, M.; Fowler, E. W.; Rawlins, J. W. Another Look at Epoxy Thermosets Correlating Structure with Mechanical Properties. *Polym. Eng. Sci.* **2014**, *54* (9), 1990–2004.

(63) Henniker, J. C. Infrared Spectrometry of Industrial Polymers. **1967**.

(64) Grdadolnik, J. ATR-FTIR Spectroscopy: Its Advantage and Limitations. *Acta Chim. Slov.* **2002**, *49* (3), 631–642.

(65) Poisson, N.; Lachenal, G.; Sautereau, H. Near-and Mid-Infrared Spectroscopy Studies of an Epoxy Reactive System. *Vib. Spectrosc.* **1996**, *12* (2), 237–247.

(66) Materazzi, S. Thermogravimetry–Infrared Spectroscopy (TG-FTIR) Coupled Analysis. *Appl. Spectrosc. Rev.* **1997**, *32* (4), 385–404.

(67) González, M. G.; Cabanelas, J. C.; Baselga, J. Applications of FTIR on Epoxy Resins-Identification, Monitoring the Curing Process, Phase Separation and Water Uptake. In *Infrared Spectroscopy-Materials Science, Engineering and Technology*; IntechOpen, 2012.

(68) Pfeiffer, H. G.; Liebhafsky, H. A. The Origins of Beer's Law. *J. Chem. Educ.* **1951**, *28* (3), 123.

(69) Berberan-Santos, M. N. Beer's Law Revisited. *J. Chem. Educ.* **1990**, *67* (9), 757.

(70) Min, B.-G.; Stachurski, Z. H.; Hodgkin, J. H.; Heath, G. R. Quantitative Analysis of the Cure Reaction of DGEBA/DDS Epoxy Resins without and with Thermoplastic Polysulfone Modifier Using near Infra-Red Spectroscopy. *Polymer (Guildf).* **1993**, *34* (17), 3620–3627.

(71) González, M.; Kindelán, M.; Cabanelas, J. C.; Baselga, J. Modelling Auto-acceleration in DGEBA/Diamine Systems. In *Macromolecular Symposia*; Wiley Online Library, 2003; Vol. 200, pp 111–120.

(72) Workman, J. A Review of Process near Infrared Spectroscopy: 1980–1994. *J. near infrared Spectrosc.* **1993**, *1* (4), 221–245.

(73) Xu, L.; Fu, J. H.; Schlup, J. R. In Situ Near-Infrared Spectroscopic Investigation of Epoxy Resin-Aromatic Amine Cure Mechanisms. *J. Am. Chem. Soc.* **1994**, *116* (7), 2821–2826.

(74) Mijović, J.; Andjelić, S.; Kenny, J. M. In Situ Real-time Monitoring of Epoxy/Amine Kinetics by Remote near Infrared Spectroscopy. *Polym. Adv. Technol.* **1996**, *7* (1), 1–16.

(75) Santos, A. F.; Silva, F. M.; Lenzi, M. K.; Pinto*, J. C. Monitoring and Control of Polymerization Reactors Using NIR Spectroscopy. *Polym. Plast. Technol. Eng.* **2005**, *44* (1), 1–61.

(76) Goddu, R. F.; Delker, D. A. Determination of Terminal Epoxides by Near-Infrared Spectrophotometry. *Anal. Chem.* **1958**, *30* (12), 2013–2016.

(77) Goddu, R. F.; Delker, D. A. Spectra-Structure Correlations for near-Infrared Region. *Anal. Chem.* **1960**, *32* (1), 140–141.

(78) Musto, P.; Martuscelli, E.; Ragosta, G.; Russo, P.; Villano, P. Tetrafunctional Epoxy Resins: Modeling the Curing Kinetics Based on FTIR Spectroscopy Data. *J. Appl. Polym. Sci.* **1999**, *74* (3), 532–540.

(79) Schiering, D. W.; Katon, J. E.; Drazal, L. T.; Gupta, V. B. An Infrared Spectroscopic Investigation of the Curing Reactions of the EPON 828/Meta-phenylenediamine System. *J. Appl. Polym. Sci.* **1987**, *34* (7), 2367–2375.

(80) St John, N. A.; George, G. A. Cure Kinetics and Mechanisms of a Tetraglycidyl-4, 4′-Diaminodiphenylmethane/Diaminodiphenylsulphone Epoxy Resin Using near Ir Spectroscopy. *Polymer (Guildf).* **1992**, *33* (13), 2679–2688.

(81) Xu, L.; Schlup, J. R. Etherification versus Amine Addition during Epoxy Resin/Amine Cure: An in Situ Study Using Near-infrared Spectroscopy. *J. Appl. Polym. Sci.* **1998**, *67* (5), 895–901.

(82) Xu, L.; Fu, J. H.; Schlup, J. R. In Situ Near-Infrared Spectroscopic Investigation of the Kinetics and Mechanisms of Reactions between Phenyl Glycidyl Ether (PGE) and Multifunctional Aromatic Amines. *Ind. Eng. Chem. Res.* **1996**, *35* (3), 963–972.

(83) Chike, K. E.; Myrick, M. L.; Lyon, R. E.; Angel, S. M. Raman and Near-Infrared Studies of an Epoxy Resin. *Appl. Spectrosc.* **1993**, *47* (10), 1631–1635.

(84) Yousefi, A.; Lafleur, P. G.; Gauvin, R. Kinetic Studies of Thermoset Cure Reactions: A Review. *Polym. Compos.* **1997**, *18* (2), 157–168.

(85) Czél, G.; Czigány, T. A Study of Water Absorption and Mechanical Properties of Glass Fiber/Polyester Composite Pipes—effects of Specimen Geometry and Preparation. *J. Compos. Mater.* **2008**, *42* (26), 2815–2827.

(86) Lloyd, W. G.; Alfrey Jr, T. Network Polymers. II. Experimental Study of Swelling. *J. Polym. Sci.* **1962**, *62* (174), 301–316.

(87) Dümichen, E.; Javdanitehran, M.; Erdmann, M.; Trappe, V.; Sturm, H.; Braun, U.; Ziegmann, G. Analyzing the Network Formation and Curing Kinetics of Epoxy Resins by in Situ Near-Infrared Measurements with Variable Heating Rates. *Thermochim. Acta* **2015**, *616*, 49–60.

(88) Estridge, C. E. The Effects of Competitive Primary and Secondary Amine Reactivity on the Structural Evolution and Properties of an Epoxy Thermoset Resin during Cure: A Molecular Dynamics Study. *Polymer (Guildf).* **2018**, *141*, 12–20.